transcriptional dysregulation. The ideal therapy for polyglutamine diseases appears to be a combination of these potential therapeutic strategies, since each drug has potential adverse effects when used in a long term (Agrawal et al., 2005). In addition to pharmacological approaches, genetic interventions such as RNA interference can be applied if safety and delivery problems are solved (Caplen et al., 2002).

Since various therapeutic strategies for SBMA have emerged thanks to animal models recapitulating human diseases, it is of utmost importance to pursue intensive clinical studies to verify the results from animal studies (Table 1). When we apply candidate agents for patients, it should be considered that the majority of therapeutics emerging form animal studies are disease-modifying therapy, but not symptom-relief (Fig. 5). Given that SBMA is a slowly progressive disease, extremely long-term clinical trials are likely necessary to verify clinical benefits of disease-modifying therapies by targeting clinical endpoints such as occurrence of aspiration pneumonia or becoming wheelchair-bound. Suitable surrogate endpoints, which reflect the pathogenesis and severity of SBMA, are thus substantial to assess the therapeutic efficacy in drug trials. To this end, appropriate biomarkers should be identified and validated in translational researches.

Acknowledgments

Fig. 2 is reproduced from Katsuno et al., "Leuprorelin rescues polyglutamine-dependent phenotypes in a transgenic mouse model of spinal and bulbar muscular atrophy (SBMA)" Nat. Med. 9: 768–773, 2003. Fig. 3 is reproduced from Waza et al., "17-AAG, an Hsp90 inhibitor, ameliorates polyglutamine-mediated motor neuron degeneration" Nat. Med. 11: 1088–1095, 2005. This work was supported by a Center-of-Excellence (COE) grant from the Ministry of Education, Culture, Sports, Science and Technology, Japan, and grants from the Ministry of Health, Labour and Welfare, Japan.

References

Adachi, H., Kume, A., Li, M., Nakagomi, Y., Niwa, H., Do, J., Sang, C., Kobayashi, Y., Doyu, M., Sobue, G., 2001. Transgenic mice with an expanded CAG repeat controlled by the human AR promoter show polyglutamine nuclear inclusions and neuronal dysfunction without neuronal cell death. Hum. Mol. Genet. 10, 1039–1048.

Adachi, H., Katsuno, M., Minamiyama, M., Sang, C., Pagoulatos, G., Angelidis, C., Kusakabe, M., Yoshiki, A., Kobayashi, Y., Doyu, M., Sobue, G., 2003. Heat shock protein 70 chaperone overexpression ameliorates phenotypes of the spinal and bulbar muscular atrophy transgenic mouse model by reducing nuclear-localized mutant androgen receptor protein. J. Neurosci. 23, 2203–2211.

Adachi, H., Katsuno, M., Minamiyama, M., Waza, M., Sang, C., Nakagomi, Y., Kobayashi, Y., Tanaka, F., Doyu, M., Inukai, A., Yoshida, M., Hashizume, Y., Sobue, G., 2005. Widespread nuclear and cytoplasmic accumulation of mutant androgen receptor in SBMA patients. Brain 128, 659–670.

Agrawal, N., Pallos, J., Slepko, N., Apostol, B.L., Bodai, L., Chang, L.W., Chiang, A.S., Thompson, L.M., Marsh, J.L., 2005. Identification of combinatorial drug regimens for treatment of Huntington's disease using *Drosophila*. Proc. Natl. Acad. Sci. U. S. A. 102, 3777–3781.

Arrasate, M., Mitra, S., Schweitzer, E.S., Segal, M.R., Finkbeiner, S., 2004. Inclusion body formation reduces levels of mutant huntingtin and the risk of neuronal death. Nature 431, 805–810.

Bailey, C.K., Andriola, I.F., Kampinga, H.H., Merry, D.E., 2002. Molecular chaperones enhance the degradation of expanded polyglutamine repeat androgen receptor in a cellular model of spinal and bulbar muscular atrophy. Hum. Mol. Genet. 11, 515–523.

Banno, H., Adachi, H., Katsuno, M., Suzuki, K., Atsuta, N., Watanabe, H., Tanaka, F., Doyu, M., Sobue, G., in press. Mutant androgen receptor accumulation in SBMA scrotal skin: a pathogenic marker. Ann. Neurol.

Batulan, Z., Shinder, G.A., Minotti, S., He, B.P., Doroudchi, M.M., Nalbantoglu, J., Strong, M.J., Durham, H.D., 2003. High threshold for induction of the stress response in motor neurons is associated with failure to activate HSF1. J. Neurosci. 23, 5789–5798.

Caplen, N.J., Taylor, J.P., Statham, V.S., Tanaka, F., Fire, A., Morgan, R.A., 2002. Rescue of polyglutamine-mediated cytotoxicity by double-stranded RNA-mediated RNA interference. Hum. Mol. Genet. 11, 175–184.

Chevalier-Larsen, E.S., O'Brien, C.J., Wang, H., Jenkins, S.C., Holder, L., Lieberman, A.P., Merry, D.E., 2004. Castration restores function and neurofilament alterations of aged symptomatic males in a transgenic mouse model of spinal and bulbar muscular atrophy. J. Neurosci. 24, 4778–4786.

Clark, P.E., Irvine, R.A., Coetzee, G.A., 2003. The androgen receptor CAG repeat and prostate cancer risk. Methods Mol. Med. 81, 255–266.

Cowan, K.J., Diamond, M.I., Welch, W.J., 2003. Polyglutamine protein aggregation and toxicity are linked to the cellular stress response. Hum. Mol. Genet. 12, 1377–1391.

Doyu, M., Sobue, G., Mukai, E., Kachi, T., Yasuda, T., Mitsuma, T., Takahashi, A., 1992. Severity of X-linked recessive bulbospinal neuronopathy correlates with size of the tandem CAG repeat in androgen receptor gene. Ann. Neurol. 32, 707–710.

Fischbeck, K.H., 1997. Kennedy disease. J. Inherited Metab. Dis. 20, 152–158.

Gatchel, J.R., Zoghbi, H.Y., 2005. Diseases of unstable repeat expansion: mechanism and principles. Nat. Rev., Genet. 6, 743–755.

Gunawardena, S., Goldstein, L.S., 2005. Polyglutamine diseases and transport problems: deadly traffic jams on neuronal highways. Arch. Neurol. 62, 46–51.

Hafezparast, M., Klocke, R., Ruhrberg, C., Marquardt, A., Ahmad-Annuar, A., Bowen, S., Lalli, G., Witherden, A.S., Hummerich, H., Nicholson, S., Morgan, P.J., Oozageer, R., Priestley, J.V., Averillm, S., King, V.R., Ball, S., Peters, J., Toda, T., Yamamoto, A., Hiraoka, Y., Augustin, M., Korthaus, D., Wattler, S., Wabnitz, P., Dickneite, C., Lampel, S., Boehme, F., Peraus, G., Popp, A., Rudelius, M., Schlegel, J., Fuchs, H., Hrabe de Angelis, M., Schiavo, G., Shima, D.T., Russ, A.P., Stumm, G., Martin, J.E., Fisher, E.M., 2003. Mutations in dynein link motor neuron degeneration to defects in retrograde transport. Science 300, 808–812.

Hay, D.G., Sathasivam, K., Tobaben, S., Stahl, B., Marber, M., Mestril, R., Mahal, A., Smith, D.L., Woodman, B., Bates, G.P., 2004. Progressive decrease in chaperone protein levels in a mouse model of Huntington's disease and induction of stress proteins as a therapeutic approach. Hum. Mol. Genet. 13, 1389–1405.

Heinlein, C.A., Chang, C., 2001. Role of chaperones in nuclear translocation and transactivation of steroid receptors. Endocrine 14, 143–149.

Hirakawa, T., Rokutan, K., Nikawa, T., Kishi, K., 1996. Geranylgeranylacetone induces heat shock proteins in cultured guinea pig gastric mucosal cells and rat gastric mucosa. Gastroenterology 111, 345–357.

Hockly, E., Richon, V.M., Woodman, B., Smith, D.L., Zhou, X., Rosa, E., Sathasivam, K., Ghazi-Noori, S., Mahal, A., Lowden, P.A., Steffan, J.S., Marsh, J.L., Thompson, L.M., Lewis, C.M., Marks, P.A., Bates, G.P., 2003. Suberoylanilide hydroxamic acid, a histone deacetylase inhibitor, ameliorates motor deficits in a mouse model of Huntington's disease. Proc. Natl. Acad. Sci. U. S. A. 100, 2041–2046.

Katsuno, M., Adachi, H., Kume, A., Li, M., Nakagomi, Y., Niwa, H., Sang, C., Kobayashi, Y., Doyu, M., Sobue, G., 2002. Testosterone reduction prevents phenotypic expression in a transgenic mouse model of spinal and bulbar muscular atrophy. Neuron 35, 843–854.

Katsuno, M., Adachi, H., Doyu, M., Minamiyama, M., Sang, C., Kobayashi, Y., Inukai, A., Sobue, G., 2003. Leuprorelin rescues polyglutamine-dependent phenotypes in a transgenic mouse model of spinal and bulbar muscular atrophy. Nat. Med. 9, 768–773.

Katsuno, M., Adachi, H., Tanaka, F., Sobue, G., 2004. Spinal and bulbar muscular atrophy: ligand-dependent pathogenesis and therapeutic perspectives. J. Mol. Med. 82, 298–307.

Katsuno, M., Sang, C., Adachi, H., Minamiyama, M., Waza, M., Tanaka, F., Doyu, M., Sobue, G., 2005. Pharmacological induction of heat-shock proteins alleviates polyglutamine-mediated motor neuron disease. Proc. Natl. Acad. Sci. U. S. A. 102, 16801–16806.

Kawahara, H., 1897. A family of progressive bulbar palsy. Aichi. Med. J. 16, 3–4 (in Japanese).

Kennedy, W.R., Alter, M., Sung, J.H., 1968. Progressive proximal spinal and bulbar muscular atrophy of late onset. A sex-linked recessive trait. Neurology 18, 671–680.

Kobayashi, Y., Miwa, S., Merry, D.E., Kume, A., Mei, L., Doyu, M., Sobue, G., 1998. Caspase-3 cleaves the expanded androgen receptor protein of spinal and bulbar muscular atrophy in a polyglutamine repeat length-dependent manner. Biochem. Biophys. Res. Commun. 252, 145–150.

Kobayashi, Y., Kume, A., Li, M., Doyu, M., Hata, M., Ohtsuka, K., Sobue, G., 2000. Chaperones Hsp70 and Hsp40 suppress aggregate formation and apoptosis in cultured neuronal cells expressing truncated androgen receptor protein with expanded polyglutamine tract. J. Biol. Chem. 275, 8772–8778.

La Spada, A.R., Wilson, E.M., Lubahn, D.B., Harding, A.E., Fischbeck, K.H., 1991. Androgen receptor gene mutations in X-linked spinal and bulbar muscular atrophy. Nature 352, 77–79.

Li, M., Miwa, S., Kobayashi, Y., Merry, D.E., Yamamoto, M., Tanaka, F., Doyu, M., Hashizume, Y., Fischbeck, K.H., Sobue, G., 1998. Nuclear inclusions of the androgen receptor protein in spinal and bulbar muscular atrophy. Ann. Neurol. 44, 249–254.

Macario, A.J., Conway de Macario, E., 2005. Sick chaperones, cellular stress, and disease. N. Engl. J. Med. 353, 1489–1501.

Mariotti, C., Castellotti, B., Pareyson, D., Testa, D., Eoli, M., Antozzi, C., Silani, V., Marconi, R., Tezzon, F., Siciliano, G., Marchini, C., Gellera, C., Donato, S.D., 2000. Phenotypic manifestations associated with CAG-repeat expansion in the androgen receptor gene in male patients and heterozygous females: a clinical and molecular study of 30 families. Neuromuscul. Disord. 10, 391–397.

Minamiyama, M., Katsuno, M., Adachi, H., Waza, M., Sang, C., Kobayashi, Y., Tanaka, F., Doyu, M., Inukai, A., Sobue, G., 2004. Sodium butyrate ameliorates phenotypic expression in a transgenic mouse model of spinal and bulbar muscular atrophy. Hum. Mol. Genet. 13, 1183–1192.

Muchowski, P.J., Wacker, J.L., 2005. Modulation of neurodegeneration by molecular chaperones. Nat. Rev., Neurosci. 6, 11–22.

Nucifora Jr., F.C., Sasaki, M., Peters, M.F., Huang, H., Cooper, J.K., Yamada, M., Takahashi, H., Tsuji, S., Troncoso, J., Dawson, V.L., Dawson, T.M., Ross, C. A., 2001. Interference by huntingtin and atrophin-1 with cbp-mediated transcription leading to cellular toxicity. Science 291, 2423–2428.

Poletti, A., 2004. The polyglutamine tract of androgen receptor: from functions to dysfunctions in motor neurons. Front. Neuroendocrinol. 25, 1–26.

Pratt, W.B., Toft, D.O., 2003. Regulation of signaling protein function and trafficking by the hsp90/hsp70-based chaperone machinery. Exp. Biol. Med. 228, 111–133.

Puls, I., Jonnakuty, C., LaMonte, B.H., Holzbaur, E.L., Tokito, M., Mann, E., Floeter, M.K., Bidus, K., Drayna, D., Oh, S.J., Brown Jr., R.H., Ludlow, C.L., Fischbeck, K.H., 2003. Mutant dynactin in motor neuron disease. Nat. Genet. 33, 455–456.

Schmidt, B.J., Greenberg, C.R., Allingham-Hawkins, D.J., Spriggs, E.L., 2002. Expression of X-linked bulbospinal muscular atrophy (Kennedy disease) in two homozygous women. Neurology 59, 770–772.

Sobue, G., Hashizume, Y., Mukai, E., Hirayama, M., Mitsuma, T., Takahashi, A., 1989. X-linked recessive bulbospinal neuronopathy. A clinicopathological study. Brain 112, 209–232.

Sobue, G., Doyu, M., Kachi, T., Yasuda, T., Mukai, E., Kumagai, T., Mitsuma, T., 1993. Subclinical phenotypic expressions in heterozygous females of X-linked recessive bulbospinal neuronopathy. J. Neurol. Sci. 117, 74–78.

Sopher, B.L., Thomas, Jr., P.S., LaFevre-Bernt, M.A., Holm, I.E., Wilke, S.A., Ware, C.B., Jin, L.W., Libby, R.T., Ellerby, L.M., La Spada, A.R., 2004. Androgen receptor YAC transgenic mice recapitulate SBMA motor neuronopathy and implicate VEGF164 in the motor neuron degeneration. Neuron 41, 687–699.

Sperfeld, A.D., Karitzky, J., Brummer, D., Schreiber, H., Haussler, J., Ludolph, A.C., Hanemann, C.O., 2002. X-linked bulbospinal neuropathy: Kennedy disease. Arch. Neurol. 59, 1921–1926.

Steffan, J.S., Bodai, L., Pallos, J., Poelman, M., McCampbell, A., Apostol, B.L., Kazantsev, A., Schmidt, E., Zhu, Y.Z., Greenwald, M., Kurokawa, R., Housman, D.E., Jackson, G.R., Marsh, J.L., Thompson, L.M., 2001. Histone deacetylase inhibitors arrest polyglutamine-dependent neurodegeneration in *Drosophila*. Nature 413, 739–743.

Sugars, K.L., Rubinsztein, D.C., 2003. Transcriptional abnormalities in Huntington disease. Trends Genet. 19, 233–238.

Szebenyi, G., Morfini, G.A., Babcock, A., Gould, M., Selkoe, K., Stenoien, D.L., Young, M., Faber, P.W., MacDonald, M.E., McPhaul, M.J., Brady, S.T., 2003. Neuropathogenic forms of huntingtin and androgen receptor inhibit fast axonal transport. Neuron 40, 41–52.

Takeyama, K., Ito, S., Yamamoto, A., Tanimoto, H., Furutani, T., Kanuka, H., Miura, M., Tabata, T., Kato, S., 2002. Androgen-dependent neurodegeneration by polyglutamine-expanded human androgen receptor in *Drosophila*. Neuron 35, 855–864.

Walcott, J.L., Merry, D.E., 2002. Ligand promotes intranuclear inclusions in a novel cell model of spinal and bulbar muscular atrophy. J. Biol. Chem. 277, 50855–50859.

Waza, M., Adachi, H., Katsuno, M., Minamiyama, M., Sang, C., Tanaka, F., Inukai, A., Doyu, M., Sobue, G., 2005. 17-AAG, an Hsp90 inhibitor, ameliorates polyglutamine-mediated motor neuron degeneration. Nat. Med. 11, 1088–1095.

Wyttenbach, A., 2004. Role of heat shock proteins during polyglutamine neurodegeneration: mechanisms and hypothesis. J. Mol. Neurosci. 23, 69–96.

Mutant Androgen Receptor Accumulation in Spinal and Bulbar Muscular Atrophy Scrotal Skin: A Pathogenic Marker

Haruhiko Banno, MD, Hiroaki Adachi, MD, Masahisa Katsuno, MD, Keisuke Suzuki, MD, Naoki Atsuta, MD, Hirohisa Watanabe, MD, Fumiaki Tanaka, MD, Manabu Doyu, MD, and Gen Sobue, MD

Objective: **Spinal and bulbar muscular atrophy (SBMA) is a hereditary motor neuron disease caused by the expansion of a polyglutamine tract in the androgen receptor (AR). The nuclear accumulation of mutant AR is central to the pathogenesis of SBMA. Androgen deprivation with leuprorelin inhibits mutant AR accumulation, resulting in rescue of neuronal dysfunction in a mouse model of SBMA. This study aimed to investigate whether mutant AR accumulation in the scrotal skin is an appropriate biomarker of SBMA.** ***Methods:*** **Immunohistochemistry of both scrotal skin and the spinal cord was performed on five autopsied SBMA cases. Neurological severity and scrotal skin findings were studied in another 13 patients. Five other patients received subcutaneous injections of leuprorelin and underwent scrotal skin biopsy.** ***Results:*** **The degree of mutant AR accumulation in scrotal skin epithelial cells tended to be correlated with that in the spinal motor neurons in autopsy specimens, and it was well correlated with CAG repeat length and inversely correlated with the amyotrophic lateral sclerosis functional scale. Leuprorelin treatment inhibited mutant AR protein accumulation in the scrotal skin of SBMA patients.** ***Interpretation:*** **These observations suggest that scrotal skin biopsy findings are a potent pathogenic marker of SBMA and can be a surrogate end point in therapeutic trials.**

Ann Neurol 2006;59:520–526

Spinal and bulbar muscular atrophy (SBMA), also known as Kennedy's disease, is an adult-onset motor neuron disease characterized by muscle atrophy, weakness, contraction fasciculations, and bulbar involvement.[1–4] SBMA exclusively affects men in their 30s or 40s, and disease progression is slow.[1,5] The molecular basis of SBMA is the expansion of a trinucleotide CAG repeat, which encodes a polyglutamine (polyQ) tract, in the androgen receptor (AR) gene.[6] The CAG repeat numbers range from 38 to 62 in SBMA patients, whereas healthy individuals have 10 to 36 CAGs.[6,7] The number of CAGs is correlated with disease severity and is inversely correlated with age of onset,[8,9] as observed in other polyQ-related neurodegenerative diseases including Huntington's disease and several forms of spinocerebellar ataxia.[10]

Histopathologically, lower motor neurons are markedly depleted in the spinal cord and brainstem, and nuclear inclusions (NIs) containing the mutant and truncated AR with expanded polyQ are present in the residual motor neurons, as well as in cells of the scrotal skin and other visceral organs.[3,11,12] Although NIs are a disease-specific pathological marker, they may reflect a cellular protective response against the toxicity of abnormal polyQ-containing protein.[13] In contrast, the therapeutic effect of testosterone deprivation in our SBMA transgenic mouse model suggested that diffuse nuclear accumulation of mutant AR is a cardinal pathogenic process underlying neurological manifestations.[14,15] This hypothesis has also been clearly illustrated by the observation that the extent of diffuse nuclear accumulation of mutant AR, but not NIs, in the motor neurons of the spinal cord was closely related to CAG repeat length in autopsied SBMA cases.[16] Nuclear localization of the mutant protein has now been considered essential for inducing neuronal cell dysfunction and degeneration in the majority of polyQ diseases.[10]

A characteristic clinical feature of SBMA is that the disease occurs in male but not female individuals, even when they are homozygous for the mutation.[17,18] Several studies have clarified that the sex dependency of disease manifestation in SBMA arises from testosterone-dependent nuclear accumulation of mu-

From the Department of Neurology, Nagoya University Graduate School of Medicine, Showa-ku, Nagoya, Japan.

Received Sep 1, 2005, and in revised form Oct 4. Accepted for publication Oct 6, 2005.

Published online Dec 15, 2005 in Wiley InterScience (www.interscience.wiley.com). DOI: 10.1002/ana.20735

Address correspondence to Dr Sobue, Department of Neurology, Nagoya University Graduate School of Medicine, 65 Tsurumai-cho, Showa-ku, Nagoya 466-8550, Japan.
E-mail: sobueg@med.nagoya-u.ac.jp

tant AR.[14,15,19,20] Leuprorelin, a leuteinizing hormone–releasing hormone agonist that reduces testosterone release from the testis and inhibits nuclear accumulation of mutant AR, rescued motor dysfunction in male transgenic mice carrying the full-length human AR with expanded polyQ.[15]

Although data from transgenic mice studies indicated that androgen deprivation from leuprorelin treatment is a potent therapeutic agent for SBMA,[14,15] clinical experience using this drug for SBMA patients is limited.[21] Because long-term clinical trials are needed to establish the efficacy of therapeutics ameliorating disease progression in slowly progressive neurodegenerative diseases such as SBMA, an appropriate biomarker reflecting pathogenic processes of the disease is necessary. The aim of this study was to test the hypothesis that peripheral accumulation of mutant AR in the scrotal skin represents a suitable biomarker of SBMA that can be applicable as a surrogate end point in therapeutic trials.

Patients and Methods

Patients

Twenty-three patients with clinically and genetically confirmed SBMA were examined. Patient characteristics are shown in the Table. Five of the 23 patients underwent autopsy, and both the scrotal skin and the spinal cord were examined; another 13 patients underwent biopsy of the scrotal skin. The remaining five patients were enrolled in a leuprorelin study and also underwent biopsy of the scrotal skin. All patients were hospitalized and underwent follow-up examinations at Nagoya University Hospital (Nagoya, Japan) and its affiliated hospitals.

For each of the 18 patients who underwent biopsy of the scrotal skin, three scrotal skin specimens were made by punch biopsy using a 3mm diameter Dermapunch (Nipro, Tokyo, Japan) under 10ml lidocaine acetate local anesthesia. All patients who underwent biopsy sterilized the wound for several days by themselves and received 4 days of cefaclor (250mg three times a day) antibiotic therapy after the procedure. The 13 patients who underwent biopsy who were not enrolled in the leuprorelin trial were also assessed on the amyotrophic lateral sclerosis functional scale (limb Norris score), as described previously.[22]

Five other male subjects (age, 60–74 years; mean, 67.3 years) who died of nonneurological diseases served as control subjects. The Nagoya University Hospital Institutional Review Board approved the collection of data and specimens, and all patients gave their written, informed consent to participate.

Leuprorelin Administration

Five patients received subcutaneous injections of 3.75mg leuprorelin once every 4 weeks. The patients, aged 43 to 68 years, were capable of walking with or without a cane and expressed no desire to father a child. They were observed for 6 months (24 weeks), and scrotal skin biopsies were taken from each patient at 0, 4, and 12 weeks after initial leuprorelin administration. Serum creatine kinase (CK) was determined by ultraviolet measurement using hexokinase and glucose-6-phosphate. Serum testosterone levels were measured by radioimmunoassay using the DPC total testosterone kit (Diagnostic Products Corporation, Los Angeles, CA).

Immunohistochemical Detection of the Mutant Androgen Receptor in the Scrotal Skin and Spinal Cord

Immunohistochemistry of scrotal skin specimens and the spinal cord were conducted as described previously.[16] In brief, we prepared 5μm-thick, formalin-fixed, paraffin-embedded sections of scrotal skin and spinal cord from SBMA patients. Sections were deparaffinized and rehydrated through a graded series of alcohol-water solutions. For the mutant AR immunohistochemical study, sections were pretreated with immersion in 98% formic acid for 5 minutes, and then with microwave oven heating for 15 minutes in 10mM citrate buffer at pH 6.0. Sections were incubated with a mouse anti-expanded polyQ antibody (1:20,000; 1C2; Chemicon, Temecula, CA)[23] to evaluate the nuclear accumulation of mutant AR.[14–16] Immune complexes were visualized using the Envision-plus kit (Dako, Glostrup, Denmark). Sections were counterstained with Mayer's hematoxylin. For electron microscopic immunohistochemistry, the sections were processed

Table. Patient Characteristics

Characteristics	Autopsy Study (N = 5)	Biopsy Alone Study (N = 13)	Leuprorelin + Biopsy Study (N = 5)
Age (mean ± SD), yr	64.8 ± 10.8	54.8 ± 9.6	50.2 ± 10.8
Duration of weakness (mean ± SD), yr	38.4 ± 14.7	11.0 ± 7.4	8.8 ± 4.9
(CAG)n (mean ± SD)	47.4 ± 4.9	48.2 ± 3.0	49.2 ± 4.9
ADL (cane/independent ratio)	NA	4/9	2/3
Limb Norris score (mean ± SD)	NA	53.4 ± 6.9	52.0 ± 6.8
Norris bulbar score (mean ± SD)	NA	32.2 ± 3.4	32.8 ± 6.2
ALSFRS-R (Japanese edition) (mean ± SD)	NA	40.3 ± 3.2	39.2 ± 3.8
Cause of death	Pneumonia (n = 4); Lung cancer (n = 1)	NA	NA

The amyotrophic lateral sclerosis functional rating scale-revised.
SD = standard deviation; (CAG)n = number of expanded CAG repeats in the SBMA allele; NA = not applicable; ADL = activities of daily living.

as described for light microscopic immunohistochemistry, and then fixed with 2% osmium tetroxide in 0.1M phosphate buffer at pH 7.4, dehydrated in graded alcohol-water solutions, and embedded in epoxy resin. Ultrathin sections were cut for observation under an electron microscope (H-7100; Hitachi High-Technologies Corporation, Tokyo, Japan).

Quantification of Cell Population with Diffuse Nuclear Staining

For quantitative assessment of scrotal skin cells, the frequency of diffuse nuclear staining was calculated from counts of more than 500 nuclei in 5 randomly selected fields of each section photographed at 400× magnification (BX51TF; Olympus, Tokyo, Japan). To assess the nuclear accumulation of mutant AR in spinal cord motor neurons, we prepared at least 100 transverse sections each from the cervical, thoracic, and lumber spinal cord for anti-expanded polyQ antibody staining with 1C2. The numbers of 1C2-positive cells in the ventral horn on both the right and left sides were counted on every 10th section under the light microscope with a computer-assisted image analyzer (BX51TF; Olympus), as described previously.[16,24] Populations of 1C2-positive cells were expressed as percentages of the total skin cell or neuronal count.

Statistical Analysis

We analyzed the data by Pearson's coefficient, Spearman's rank correlation, and Student's paired t test as appropriate using StatView software (version 5; Hulinks, Tokyo, Japan) and considering p values less than 0.05 to be indicative of significance.

Results

Mutant Androgen Receptor Nuclear Accumulation in the Scrotal Skin and Spinal Motor Neuron

In the five autopsied cases, mutant AR nuclear accumulations were clearly visualized with anti-expanded polyQ immunostaining with 1C2 in the scrotal skin and spinal cord specimens (Fig 1A). Pathological accumulation of mutant AR was distributed in all layers of the epithelium. Diffuse nuclear accumulations were predominantly observed, and the occurrence of NIs was less frequent. This was also the case in the spinal cord specimens. Electron microscopic immunohistochemistry with the 1C2 antibody demonstrated granular dense and amorphous aggregates corresponding to diffuse nuclear staining in both spinal motor neurons and epithelial cells of scrotal skin (see Figs 1B, C). Filamentous structures such as those reported in Huntington's disease,[25] dentatorubal-pallidoluysian atrophy (DRPLA),[26] and Machado–Joseph disease[27] were not seen. No diffuse nuclear staining was seen in the control subjects. The extent of mutant AR accumulation in the scrotal skin epithelial cells showed a tendency to correlate with that in the anterior horn cells ($r = 0.84$; $p = 0.08$; see Fig 1D). Mutant AR accumulation was remarkable in both the spinal motor neurons and the scrotal skin of Patient 1, but was far less remarkable in Patient 2 (see Figs 1A, D).

Correlations of the Mutant Androgen Receptor Accumulation in the Scrotal Skin to CAG Repeat Length and Amyotrophic Lateral Sclerosis Score

Mutant AR nuclear accumulations in scrotal skin biopsies from the 13 SBMA patients who did not receive leuprorelin were assessed by 1C2 antibody staining of expanded PolyQ. The 1C2-positive cell population in the scrotal skin biopsies was significantly correlated with CAG repeat length ($r = 0.61$; $p = 0.03$; Fig 2A) and was inversely correlated with the functional scale assessed by the Norris score on limbs ($r = -0.63$; $p = 0.02$; see Fig 2B).

Leuprorelin Treatment Depletes Mutant Androgen Receptor Accumulation in the Scrotal Skin

In all five patients in which leuprorelin was administered (see the Table), both the intensity and the frequency of diffuse nuclear 1C2 staining in the scrotal epithelial cells was decreased after the first 4 weeks of administration compared with the preadministration values, and this effect was markedly enhanced after 12 weeks of treatment (Figs 3A, B). Quantitative analysis demonstrated a significant decrease in the frequency of 1C2-positive cells both 4 and 12 weeks after the initiation of leuprorelin treatment ($p < 0.01$) (see Fig 3C). Serum testosterone levels decreased to the castration level after 1 to 2 months of treatment (see Fig 3D), and serum CK values were also significantly decreased in all patients (see Fig 3D).

None of the patients showed the hot flush or obesity often reported in leuprorelin trials for prostate cancer. Although a loss of sexual function including erectile disorder was observed in all patients, no patients experienced depression. No marked exacerbations were observed in total cholesterol, triglyceride, fasting blood sugar, or HbA1c (data not shown). We could not find significant motor function changes assessed by amyotrophic lateral sclerosis functional scores in 24 weeks, but three of the five enrolled patients expressed apparent subjective improvement.

Discussion

This study demonstrated that scrotal skin biopsy with anti-expanded polyQ staining is a strong candidate for an appropriate biomarker with which to monitor SBMA pathogenic processes. Previous studies showed that the severity and progression of motor dysfunction and abatement of abnormalities in mice that were castrated or given leuprorelin paralleled the extent of diffuse nuclear mutant AR accumulation in their spinal motor neurons.[14,15] Furthermore, we demonstrated previously a significant, close correlation between the length of CAG repeat expansion and frequency of dif-

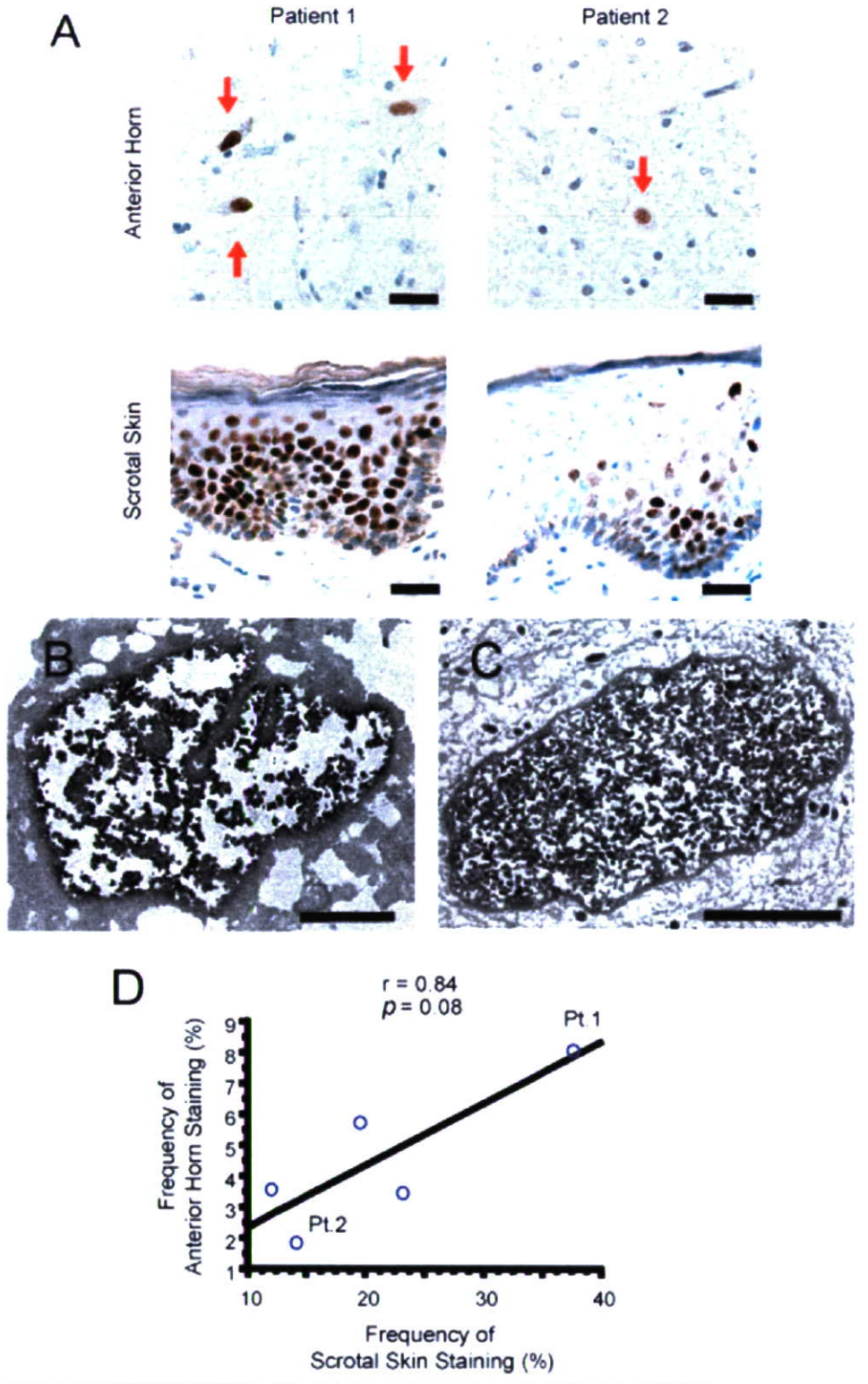

Fig 1. Mutant androgen receptor (AR) nuclear accumulation in scrotal skin and spinal motor neurons. (A) Mutant AR accumulation was remarkable in both spinal motor neurons (arrows) and scrotal skin of Patient 1, but was less remarkable in both motor neurons (arrows) and skin in Patient 2. Bar = 30μm. (B, C) Electron microscopic immunohistochemistry for 1C2 demonstrated granular dense and amorphous aggregates corresponding to diffuse nuclear staining in both spinal motor neurons and epithelial cells of scrotal skin. Bar =3μm. (D) The extent of mutant AR accumulation in scrotal skin epithelial cells showed a tendency to correlate with that in anterior horn cells. Circles (Pt. 1, Pt. 2) correspond to Patient 1 and 2 in Fig 1A.

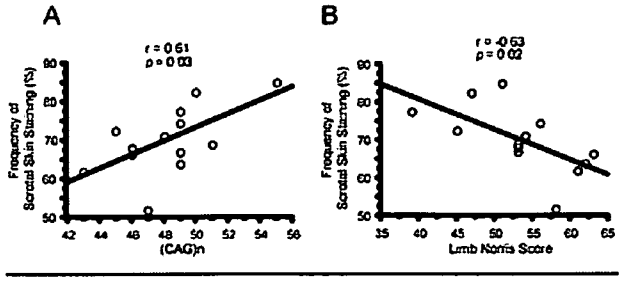

Fig 2. Correlation of the frequency of scrotal skin staining to CAG repeats and limb Norris score. The frequency of 1C2-positive cells in the scrotal skin biopsies correlated significantly with (A) CAG repeat length and (B) inversely correlated with the amyotrophic lateral sclerosis functional scale assessed by the Norris score on limbs. (CAG)n = number of expanded CAG repeats in the spinal and bulbar muscular atrophy allele.

fuse nuclear mutant AR accumulation, but not that of NIs, in the spinal cord.[16] Accordingly, neuronal dysfunction is likely to be caused by diffuse nuclear accumulation of mutant AR in the affected tissues. In this study, the extent of mutant AR nuclear accumulation in scrotal skin cells paralleled that in the anterior horn cells in autopsied cases. Electron microscopic immunohistochemistry for 1C2 anti-expanded PolyQ demonstrated granular dense and amorphous aggregates corresponding to diffuse nuclear staining in both spinal motor neurons and epithelial cells of scrotal skin. Furthermore, the fine structure of the aggregates in spinal motor neurons and epithelial cells was quite similar. Biopsy analyses in this study also suggested that scrotal skin findings were correlated with the motor functional scores of SBMA patients.

Our findings suggest that nuclear mutant AR assessed by 1C2 immunostaining in the scrotal skin is a practical procedure to estimate the severity of SBMA pathogenesis in the nervous system. In support of this view, decreases in mutant AR accumulation in the motor neurons paralleled that in nonneuronal cells in the androgen deprivation therapy tested in the mouse model of SBMA. In addition, leuprorelin treatment markedly reduced serum testosterone levels, as well as nuclear accumulation of mutant AR in the scrotal skin, suggesting that medical castration with leuprorelin intervenes in the pathogenic process of human SBMA, as demonstrated in the animal study. Moreover, serum CK levels were significantly decreased in this leuprorelin study. Because high CK values are common in SBMA patients and histopathological examinations have shown myogenic changes together with neurogenic findings in this disease,[1,3] presumably, a decrease in CK values with leuprorelin treatment implies muscular protection. Serum CK levels, however, did not significantly correlate with the Norris score on limbs or with scrotal skin biopsy findings in our cross-sectional study.

As defined by the Biomarkers Definitions Working Group, a disease biomarker should be objectively measurable and evaluated as an indicator of pathogenic processes or pharmacological responses to a therapeutic intervention.[28] Based on the observations described earlier, 1C2-stained mutant AR accumulation in the biopsied scrotal skin is likely to be a potent biomarker reflecting pathogenic processes of SBMA. Particularly, the correlation of the extent of mutant AR nuclear accumulation in the spinal motor neurons with that in scrotal skin biopsies in the autopsied cases suggests that findings in the scrotal skin can predict pathogenic processes in the motor neurons.

Although its precise natural history has not been evaluated, SBMA is a slowly progressive disease.[1,5] Thus, extremely long-term clinical trials are necessary to assess whether certain drugs can alter the natural disease progression by targeting clinical end points such as occurrence of aspiration pneumonia or becoming wheelchair bound. Suitable surrogate end points, which reflect the pathogenesis and severity of SBMA, are substantial to assess the therapeutic efficacy in drug trials. Although it is not practical to obtain biopsy specimens from the central nervous system (CNS), a punch biopsy of the scrotal skin enables a safe and accessible examination for patients.

It has also been suggested that reliance on surrogate end points can be misleading because they may not accurately predict the actual effects that treatments have on the health of a patient, as was seen with the CD4 counts in human immunodeficiency virus trials, the bone mineral density in osteoporosis trials, and others.[29] However, several factors have been suggested to consider the decision to rely on a surrogate.[30] In SBMA, mutant AR accumulation assessed by scrotal skin biopsy can be a candidate for a surrogate end point in light of several pieces of evidence. First, a credible SBMA animal model demonstrated dramatic functional motor recovery in response to testosterone deprivation therapy that depleted mutant AR accumulation in the central nervous system, as well as in nonneuronal tissues.[14,15] Second, the degree of diffuse nuclear accumulation of mutant AR in both the CNS and scrotal skin correlates well with CAG repeat length and disease severity, indicating that it is a natural phenomenon of and reflects the underlying pathology of the disease. Third, autopsy studies show that levels of nuclear AR accumulation in the scrotal skin are correlated with those in the CNS. Moreover, levels of nuclear translocated mutant AR in the scrotal skin decreased significantly in response to drug therapy that has been shown to deplete such accumulations in the CNS of SBMA mice, to significantly rescue motor dysfunction in these mice, and to partially stabilize neurological symptoms in one reported case of human SBMA.[21]

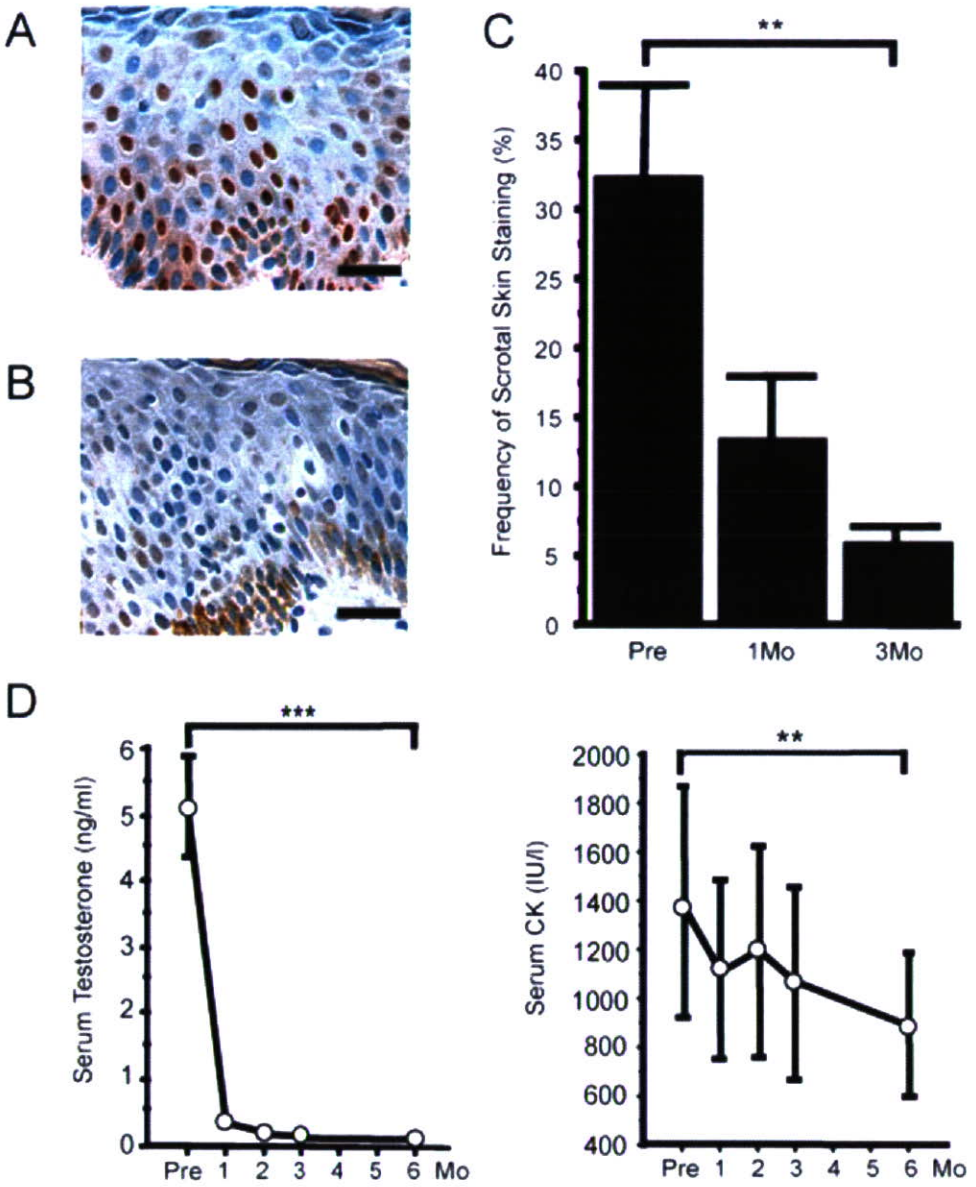

Fig 3. Effects of leuprorelin on mutant androgen receptor (AR) accumulation in scrotal skin, serum testosterone, and creatine kinase (CK). (A) Scrotal skin shows intense and frequent staining for anti-polyglutamine antibody in the nucleus before therapy. (B) Twelve weeks after therapy, both intensity and frequency of nuclear staining markedly decreased. Bar = 30μm. (C) Quantitative analysis of immunohistochemistry demonstrated a significant decrease in the number of positively stained nuclei. (D) Serum testosterone and CK decreased significantly in 6 months. Frequency of staining was calculated from counts of more than 500 nuclei in randomly selected areas and was expressed as mean ± standard deviation for 5 patients. $^{**}p < 0.01$; $^{***}p < 0.0001$.

Although our results were obtained from a small sample, nuclear accumulation of mutant AR in the scrotal skin appears to be a potent pathogenic biomarker of SBMA. A correlation between decline in validated clinical scales and nuclear mutant AR accumulations must be demonstrated in a longitudinal study to verify this histopathological feature as a biomarker for clinical severity. Similarly, validation of the scrotal skin biopsy findings as a surrogate end point in clinical trials will require a longitudinal study verifying that suppression of nuclear staining correlates with improvement on a validated clinical scale and the true clinical outcome events such as the need for a wheelchair, the presence of aspiration pneumonia, or death.

This work was supported by grants from the Ministry of Education, Culture, Sports, Science and Technology, Japan (17204032, G. S., M. D., F. T.); the Ministry of Health, Labor and Welfare, Japan (H-15-Kokoro-020, G. S., M. D.); and the Center for Clinical Trials, Japan Medical Association (G.S.).

We thank Dr N. Hishikawa for technical assistance.

References

1. Kennedy WR, Alter M, Sung JH. Progressive proximal spinal and bulbar muscular atrophy of late onset: a sex-linked recessive trait. Neurology 1968;18:671–680.
2. Sperfeld AD, Karitzky J, Brummer D, et al. X-linked bulbospinal neuropathy: Kennedy disease. Arch Neurol 2002;59: 1921–1926.
3. Sobue G, Hashizume Y, Mukai E, et al. X-linked recessive bulbospinal neuronopathy: a clinicopathological study. Brain 1989; 112:209–232.
4. Katsuno M, Adachi H, Tanaka F, et al. Spinal and bulbar muscular atrophy (SBMA): ligand-dependent pathogenesis and therapeutic perspective. J Mol Med 2004;82:298–307.
5. Sobue G, Adachi H, Katsuno M. Spinal and bulbar muscular atrophy (SBMA). In: Dickinson D, ed. Neurodegeneration: the molecular pathology of dementia and movement disorders. Basel: INS Neuropathology, 2003:275–279.
6. La Spada AR, Wilson EM, Lubahn DB, et al. Androgen receptor gene mutations in X-linked spinal and bulbar muscular atrophy. Nature 1991;352:77–79.
7. Tanaka F, Doyu M, Ito Y, et al. Founder effect in spinal and bulbar muscular atrophy (SBMA). Hum Mol Genet 1996;5: 1253–1257.
8. Doyu M, Sobue G, Mukai E, et al. Severity of X-linked recessive bulbospinal neuronopathy correlates with size of the tandem CAG repeat in androgen receptor gene. Ann Neurol 1992; 32:707–710.
9. Shimada N, Sobue G, Doyu M, et al. X-linked recessive bulbospinal neuronopathy: clinical phenotypes and CAG repeat size in androgen receptor gene. Muscle Nerve 1995;18: 1378–1384.
10. Zoghbi HY, Orr HT. Glutamine repeats and neurodegeneration. Annu Rev Neurosci 2000;23:217–247.
11. Li M, Miwa S, Kobayashi Y, et al. Nuclear inclusions of the androgen receptor protein in spinal and bulbar muscular atrophy. Ann Neurol 1998;44:249–254.
12. Li M, Nakagomi Y, Kobayashi Y, et al. Nonneural nuclear inclusions of androgen receptor protein in spinal and bulbar muscular atrophy. Am J Pathol 1998;153:695–701.
13. Arrasate M, Mitra S, Schweitzer ES, et al. Inclusion body formation reduces levels of mutant huntingtin and the risk of neuronal death. Nature 2004;431:805–810.
14. Katsuno M, Adachi H, Kume A, et al. Testosterone reduction prevents phenotypic expression in a transgenic mouse model of spinal and bulbar muscular atrophy. Neuron 2002;35: 843–854.
15. Katsuno M, Adachi H, Doyu M, et al. Leuprorelin rescues polyglutamine-dependent phenotypes in a transgenic mouse model of spinal and bulbar muscular atrophy. Nat Med 2003; 9:768–773.
16. Adachi H, Katsuno M, Minamiyama M, et al. Widespread nuclear and cytoplasmic accumulation of mutant androgen receptor in SBMA patients. Brain 2005;128:659–670.
17. Sobue G, Doyu M, Kachi T, et al. Subclinical phenotypic expressions in heterozygous females of X-linked recessive bulbospinal neuronopathy. J Neurol Sci 1993;117:74–78.
18. Schmidt BJ, Greenberg CR, Allingham-Hawkins DJ, Spriggs EL. Expression of X-linked bulbospinal muscular atrophy (Kennedy disease) in two homozygous women. Neurology 2002;59:770–772.
19. Takeyama K, Ito S, Yamamoto A, et al. Androgen-dependent neurodegeneration by polyglutamine-expanded human androgen receptor in Drosophila. Neuron 2002;35:855–864.
20. Chevalier-Larsen ES, O'Brien CJ, Wang H, et al. Castration restores function and neurofilament alterations of aged symptomatic males in a transgenic mouse model of spinal and bulbar muscular atrophy. J Neurosci 2004;24:4778–4786.
21. Shimohata T, Kimura T, Nishizawa M, et al. Five year follow up of a patient with spinal and bulbar muscular atrophy treated with leuprorelin. J Neurol Neurosurg Psychiatry 2004;75: 1206–1207.
22. Norris FH Jr, Calanchini PR, Fallat RJ, et al. The administration of guanidine in amyotrophic lateral sclerosis. Neurology 1974;24:721–728.
23. Trottier Y, Lutz Y, Stevanin G, et al. Polyglutamine expansion as a pathological epitope in Huntington's disease and four dominant cerebellar ataxias. Nature 1995;378:403–406.
24. Terao S, Sobue G, Hashizume Y, et al. Age-related changes in human spinal ventral horn cells with special reference to the loss of small neurons in the intermediate zone: a quantitative analysis. Acta Neuropathol (Berl) 1996;92:109–114.
25. DiFiglia M, Sapp E, Chase KO, et al. Aggregation of huntingtin in neuronal intranuclear inclusions and dystrophic neurites in brain. Science 1997;277:1990–1993.
26. Hayashi Y, Kakita A, Yamada M, et al. Hereditary dentatorubral-pallidoluysian atrophy: ubiquitinated filamentous inclusions in the cerebellar dentate nucleus neurons. Acta Neuropathol (Berl) 1998;95:479–482.
27. Paulson HL, Perez MK, Trottier Y, et al. Intranuclear inclusions of expanded polyglutamine protein in spinocerebellar ataxia type 3. Neuron 1997;19:333–344.
28. Biomarkers Definitions Working Group. Biomarkers and surrogate endpoints: preferred definitions and conceptual framework. Clin Pharmacol Ther 2001;69:89–95.
29. Fleming TR, DeMets DL. Surrogate end points in clinical trials: are we being misled? Ann Intern Med 1996;125: 605–613.
30. Temple R. Are surrogate markers adequate to assess cardiovascular disease drugs? JAMA 1999;282:790–795.

International Immunology, Vol. 18, No. 2, pp. 399–407
doi:10.1093/intimm/dxh379

Abnormal T cell activation caused by the imbalance of the IL-1/IL-1R antagonist system is responsible for the development of experimental autoimmune encephalomyelitis

Taizo Matsuki[1], Susumu Nakae[2], Katsuko Sudo[3], Reiko Horai[4] and **Yoichiro Iwakura**

Center for Experimental Medicine, Institute of Medical Science, University of Tokyo, Minato-ku, Tokyo 108-8639, Japan

[1]Present address: ERATO Yanagisawa Orphan Receptor Project, Japan Science and Technology Agency, Koto-ku, Tokyo 135-0064, Japan
[2]Present address: Department of Pathology, Stanford University School of Medicine, Stanford, CA 94305-5176, USA
[3]Present address: Animal Research Center, Tokyo Medical University, Sinjyuku-ku, Tokyo 160-8402, Japan
[4]Present address: National Human Genome Research Institute, National Institutes of Health, Bethesda, MD 20892, USA

Keywords: autoimmunity, cytokines, dendritic cells, knockout mouse, T cells

Abstract

IL-1 is a pro-inflammatory cytokine that plays an important role in inflammation and host responses to infection. We have previously shown that imbalances in the IL-1 and IL-1R antagonist (IL-1Ra) system cause the development of inflammatory diseases. To explore the role of the IL-1/IL-1Ra system in autoimmune disease, we analyzed myelin oligodendrocyte glycoprotein (MOG)-induced experimental autoimmune encephalomyelitis (EAE) in mice bearing targeted disruptions of the IL-1α, IL-1β, IL-1α and IL-1β (IL-1) or IL-1Ra genes. IL-1α/β double-deficient (IL-$1^{-/-}$) mice exhibited significant resistance to EAE induction with a significant reduction in disease severity, while IL-$1\alpha^{-/-}$ or IL-$1\beta^{-/-}$ mice developed EAE in a manner similar to wild-type mice. IL-$1Ra^{-/-}$ mice also developed MOG-induced EAE normally with pertussis toxin (PTx) administration. In contrast to wild-type mice, however, these mice were highly susceptible to EAE induction in the absence of PTx administration. We found that both IFN-γ and IL-17 production and proliferation were reduced in IL-$1^{-/-}$ T cells upon stimulation with MOG, while IFN-γ, IL-17 and tumor necrosis factor-α production and proliferation were enhanced in IL-$1Ra^{-/-}$ T cells. These observations suggest that the IL-1/IL-1Ra system is crucial for auto-antigen-specific T cell induction and contributes to the development of EAE.

Introduction

Multiple sclerosis (MS) is a chronic inflammatory disease associated with the demyelination of the central nervous system (CNS). Approximately, one million individuals in the world are afflicted by MS (1). Although significant progress has been made elucidating the causes of MS and improving patient outcomes over the past decade (2), definitive therapies either reducing the number of attacks or slowing the progression of disease are not yet available.

Experimental autoimmune encephalomyelitis (EAE) is regarded as an animal model mimicking several aspects of the pathogenesis of human MS, which is clinically characterized by paralysis and lethargy (3). Immunization with self-neuronal antigens, such as MBP, myelin-associated glycoprotein, proteolipid protein or myelin oligodendrocyte glycoprotein (MOG) (3, 4), results in inflammation within the CNS primarily mediated by $CD4^+$ T_h1 cells (1, 2).

Systemic or local induction of cytokines is critical in the initiation, enhancement or perpetuation of CNS disease (5). T_h1 cell-derived IFN-γ, which contributes to the etiology of a wide range of diseases, is markedly elevated within the CNS during EAE. IFN-γ-deficient and IFN-$\gamma R^{-/-}$ mice, however, remain highly susceptible to EAE (6–9). In fact, the over-expression of IFN-γ in the CNS ameliorated the severity of EAE (10). Tumor necrosis factor (TNF)α, a potent pro-inflammatory

Correspondence to: Y. Iwakura; E-mail: iwakura@ims.u-tokyo.ac.jp

Transmitting editor: Okumura

Received 5 September 2005, *accepted* 30 November 2005

Advance Access publication 13 January 2006

cytokine, is produced by a variety of cell types, including T_h1 cells. Mice over-expressing TNFα within the CNS exhibit neuronal demyelination (11, 12), while the development of EAE in $TNF\alpha^{-/-}$ mice is partially suppressed (13, 14). Other group reported, however, that in $TNF\alpha^{-/-}$ mice, the course of EAE was exacerbated by the abnormal regression and expansion of myelin-specific T cells (15). Clinically, anti-TNF therapy resulted in more severe MS (16). Thus, the contribution of pro-inflammatory cytokines, such as IFN-γ and TNFα, cannot fully explain the precise molecular mechanisms underlying EAE development.

IL-1 is produced by a variety of cells, including monocytes/macrophages, epithelial and endothelial cells and glial cells (17). Through the up-regulation of intracellular adhesion molecule-1 and vascular cell adhesion molecule-1 expression, this cytokine plays a crucial role in leukocyte extravasation into inflammatory sites (18). Dysregulation of IL-1 function leads to autoimmune and abnormal immune responses, such as arthritis and aortitis in mouse models (19, 20). Furthermore, exogenous IL-1 administration exacerbated the course of EAE, while administration of soluble IL-1R type-I (IL-1RI) or IL-1R antagonist (IL-1Ra) significantly suppressed EAE in Lewis rats (21, 22). Consistent with these observations, mice deficient in IL-1RI or IL-1R-associated kinase 1, which is involved in IL-1-mediated signal transduction, fail to develop inflammatory lesions or any evidence of EAE (23). These observations suggest that IL-1 may initiate or promote local and/or systemic inflammation during EAE pathogenesis. *In vitro*, IL-1 can augment the activation of encephalitogenic T lymphocytes, contributing to the development of EAE induced by adoptive transfer (24). Thus, IL-1 likely contributes to the activation of auto-antigen-specific immune cells, including T cells. Indeed, IL-1 can influence antigen-specific T cell activation directly (25) or indirectly via modulation of dendritic cell (DC) function (26). The importance of IL-1 in DC function, including migration, activation and acquisition of T_h1-inducing ability, has been demonstrated previously (27, 28). The precise effect of IL-1 on DCs and/or T cells during the development of EAE, however, has yet to be elucidated.

In this report, we investigate the contribution of IL-1 to the development of EAE using $IL\text{-}1^{-/-}$ and $IL\text{-}1Ra^{-/-}$ mice. We determined that IL-1 is responsible for the induction of autoreactive T cells. Our data provide evidence that the IL-1/IL-1Ra system is critical for the development of CNS autoimmune disease by modulating T cell-mediated immunity.

Methods

Mice

$IL\text{-}1\alpha^{-/-}$, $IL\text{-}1\beta^{-/-}$, $IL\text{-}1\alpha/\beta^{-/-}$ ($IL\text{-}1^{-/-}$) and $IL\text{-}1Ra^{-/-}$ mice were generated as described (29). Mice were backcrossed to the C57BL/6 strain mice for eight generations. C57BL/6 mice (wild-type mice) were purchased from Clea (Tokyo, Japan). Age- and gender-matched wild-type mice were used as controls in each experiment. Mice were kept under specific pathogen-free conditions in an environmentally controlled clean room at the Center for Experimental Medicine, Institute of Medical Science, University of Tokyo. Animals were housed in an ambient temperature of 24°C on a daily cycle of 12 h of light and darkness (8:00 a.m. to 8:00 p.m.). All the experiments were performed according to the institutional ethical guidelines for animal experimentation.

MOG peptide

MOG 35–55 (MEVGWYRSPFSRVVHLYRNGK), corresponding to the murine sequence, was synthesized on a peptide synthesizer using fluorenylmethoxycarbonyl chemistry and purified by HPLC by Ohmi (Institute of Medical Science, University of Tokyo, Japan).

Induction and evaluation of EAE

Eight- to twelve-week-old mice were subcutaneously immunized with 100 μg MOG 35–55 emulsified in CFA (1 : 1) supplemented with 400 μg *Mycobacterium tuberculosis* H37RA (DIFCO Lab., Detroit, MI, USA) in both flanks. Pertussis toxin (PTx) (500 ng) (Alexis Corp., San Diego, CA, USA) was injected intravenously into animals on the day of immunization as well as 2 days later.

Mice were inspected daily for the clinical signs of EAE for up to 30 days after immunization. Scores were determined on a scale of 0–5: 0, no disease; 1, limp tail; 2, hind limb weakness; 3, hind limb paralysis; 4, hind and fore limb paralysis and 5, moribund state. The mean clinical score was calculated by averaging the score of all of the mice in each group, including animals that did not develop EAE.

Titer for anti-MOG antibodies in serum

Detection of anti-MOG 35–55 antibodies was performed as described (25) with the following modifications. Briefly, MOG 35–55 peptide (0.5 μg per 96 well) was coated onto 96-well plates and incubated at 4°C overnight. After substantial washing and blocking, diluted sera (30 μl per well) were added to the wells for 2 h at room temperature. A series of serum dilutions were examined in preliminary experiments. After washing, alkaline phosphatase-conjugated goat anti-mouse Igs (Zymed, San Francisco, CA, USA) were added for 1 h at room temperature, followed by incubation in *p*-nitrophenyl phosphate substrate (Sigma–Aldrich, St Louis, MO, USA) as the substrate. The anti-MOG antibody titer is given as an OD_{415} value. Samples were measured in duplicate.

T cell and DC purification and proliferation assay

Mice were immunized subcutaneously with 100 μg MOG 35–55 emulsified CFA (1 : 1) with or without PTx. Ten days later, T cells were prepared from multiple lymph nodes (LNs) (axillary, inguinal, branchial, cervical and poplitial). Cells were washed, treated with anti-mouse Thy1.2 magnetic beads (Miltenyi Biotec, Bergisch Gladbach, Germany) and passed through a MACS® column to collect $Thy1.2^+$ T cells.

DCs were prepared from the spleen. Spleens were collected, minced and digested with 1 mg ml^{-1} collagenase (Sigma–Aldrich) and 1 mg ml^{-1} DNase I (Sigma–Aldrich) in HBSS for 30 min at 37°C. Following the addition of EDTA (20 mM final concentration), cells were incubated for 5 min at room temperature, passed through a 70-μm nylon mesh, layered over RPMI 1640–10% FCS–14.5% metrizamide (Cedarlane Labs., Ontario, Canada) and centrifuged at room temperature for 30 min at 500 × *g*. The low buoyant density cells at the

interface were collected and washed twice. Cells were then treated with anti-mouse CD11c magnetic beads (Miltenyi Biotec) and passed through a MACS® column. The positively selected fraction was collected, washed and re-suspended for use.

Purified DCs (1×10^4 cells) in the presence or absence of T cells (1×10^5 cells) were plated on 96-well plates coated with MOG 35–55 in a final volume of 200 µl RPMI 1640–10% FCS. After 72 h of culture, cells were pulsed with [^{3}H]thymidine ([^{3}H]TdR) (0.25 µCi ml^{-1}; Amersham Biosciences, Tokyo, Japan) for 6 h. Cells were then harvested with a Micro 96 cell harvester (Skatron, Lier, Norway). The incorporated [^{3}H]TdR radioactivity was measured using a Micro Beta System (Amersham Biosciences, Piscataway, NJ, USA). Culture supernatants were collected prior to [^{3}H]TdR incorporation to measure cytokines levels.

ELISA of cytokine levels

The levels of IL-4, IL-17 and TNFα were measured as described (30, 31). IFN-γ levels were measured with OptEIA® Set mouse IFN-γ kit (BD PharMingen). All assays were done in duplicate.

Statistical analysis

All values were calculated as the average ± SD. Comparisons were made using the Student's *t*-test, one-way analysis of variance (ANOVA), Fisher's protected least significant difference test and Mann–Whitney's *U*-test. Differences among the three groups were tested by Kruskal–Wallis one-way ANOVA.

Results

IL-1$^{-/-}$ mice are resistant to EAE

To examine the role of the IL-1/IL-1Ra system in the development of EAE, we immunized C57BL/6 wild-type, IL-1$^{-/-}$ and IL-1RI$^{-/-}$ mice with MOG 35–55 emulsified in CFA. Following the injection of PTx on days 0 and 2, the clinical signs of EAE were monitored daily and scored as described in Methods. IL-1RI$^{-/-}$ mice are known to demonstrate resistance to the development of EAE (23), suggesting that IL-1 is involved in EAE pathogenesis. We confirmed that IL-1$^{-/-}$ mice exhibit significant resistance to EAE and that IL-1RI$^{-/-}$ mice demonstrate a reduction in disease severity (Fig. 1A and data not shown) (23). The onset of EAE in IL-1$^{-/-}$ mice was also delayed from that of wild-type mice (Table 1). In contrast, mice deficient in either IL-1α or IL-1β developed EAE with a comparable severity and time course to wild-type mice (Fig. 1B). The incidence of disease, day of onset and maximal clinical score were not significantly different between wild-type, IL-1α$^{-/-}$ and IL-1β$^{-/-}$ mice (Table 1). All genotypes mice exhibited >90% disease incidence. These observations suggest that, while IL-1 plays a principal role in the development of EAE, the presence of either IL-1α or IL-1β alone is sufficient to initiate development of the disease.

Development of EAE is exacerbated in IL-1Ra$^{-/-}$ mice without PTx administration

We immunized IL-1Ra$^{-/-}$ mice with MOG 35–55 emulsified in CFA. After an injection of PTx on days 0 and 2, IL-1Ra$^{-/-}$ mice developed EAE that was comparable in time of onset and

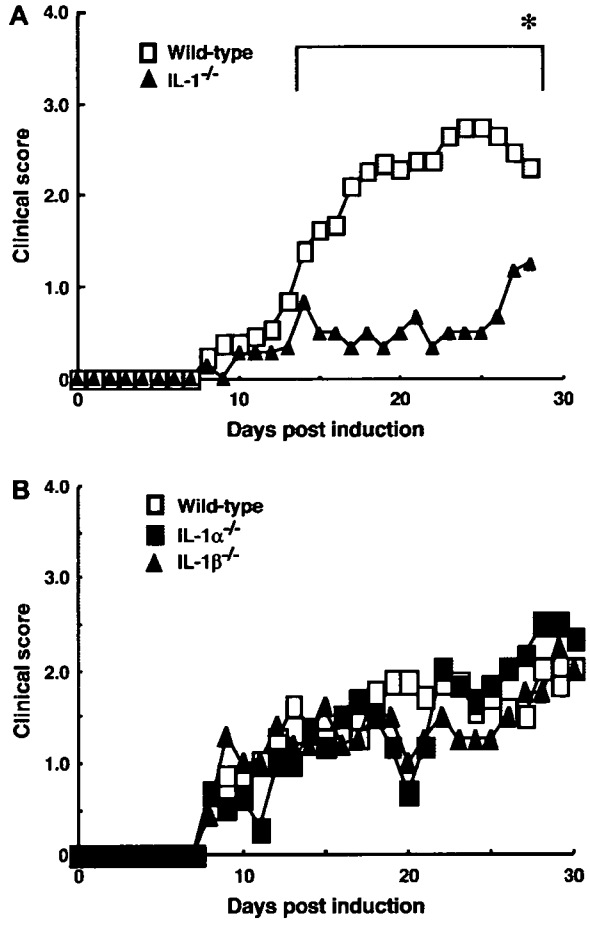

Fig. 1. Attenuated EAE induction in IL-1$^{-/-}$ mice. The clinical scores after EAE induction were determined as described in Methods. The averages of clinical scores are shown from the day of MOG immunization (day 0) to day 28 post-immunization in (A) wild-type (open squares, $n = 9$) and IL-1$^{-/-}$ (filled triangles, $n = 7$) mice and (B) wild-type (open squares, $n = 8$), IL-1α$^{-/-}$ (filled squares, $n = 9$) and IL-1β$^{-/-}$ (filled triangles, $n = 7$) mice. The data indicate the averages of each group. Statistical significances were determined by Mann–Whitney's *U*-test (A) and Kruskal–Wallis one-way ANOVA (B). *$P < 0.05$ versus wild-type mice.

severity to the EAE course observed in wild-type mice (Fig. 2A and Table 1). PTx is routinely used to facilitate the induction of experimental autoimmune diseases in animals. Previous reports using IL-10$^{-/-}$ and TNFα$^{-/-}$ mice suggested that co-administration of PTx veiled the effects of cytokines as an inflammatory factor in EAE (15, 32, 33). Therefore, to address the contribution of IL-1Ra to EAE without the complications of PTx co-administration, we examined the susceptibility of wild-type and IL-1Ra$^{-/-}$ mice to EAE in the absence of PTx. The severity of EAE was reduced in wild-type mice that were not treated with PTx (Fig. 2B). IL-1Ra$^{-/-}$ mice, however, developed severe EAE in both the absence and presence of PTx (Fig. 2B). Without PTx, IL-1Ra$^{-/-}$ mice developed more severe EAE at earlier time points than wild-type mice (Table 1). These results indicate that dysfunction of IL-1 signaling mediated by IL-1Ra deficiency contributes to EAE induction in the absence of PTx. In wild-type mice, PTx may be necessary to overcome the function of IL-1 in EAE induction.

Table 1. Clinical features of MOG 35–55-induced EAE in IL-$1^{-/-}$ and IL-$1Ra^{-/-}$ mice

	Mice	Incidence (lost)	Day of onset (average ± SD)	Maximal clinical score (average ± SD)
With PTx				
Experiment 1	Wild type	9/9 (2)	8.7 ± 0.9	3.5 ± 1.0
	IL-$1^{-/-}$	6/7 (1)	12.4 ± 4.3*	1.6 ± 1.1*
Experiment 2	Wild type	8/8 (2)	8.3 ± 0.9	2.8 ± 1.2
	IL-$1\alpha^{-/-}$	9/9 (3)	9.8 ± 1.3	2.6 ± 0.7
	IL-$1\beta^{-/-}$	6/7 (3)	8.5 ± 0.6	2.9 ± 1.7
Experiment 3	Wild type	13/13 (4)	9.2 ± 1.3	3.1 ± 1.0
	IL-$1Ra^{-/-}$	12/12 (4)	8.9 ± 1.2	3.1 ± 1.2
Without PTx				
Experiment 4	Wild type	8/8 (0)	12.8 ± 3.6	2.0 ± 0.8
	IL-$1Ra^{-/-}$	9/9 (1)	9.7 ± 0.7*	2.9 ± 0.6*

EAE was induced and scored as described in Methods. Incidence data represent the number of mice. *$P < 0.01$ versus wild-type mice of each experiment (by Student's *t*-test or one-way ANOVA).

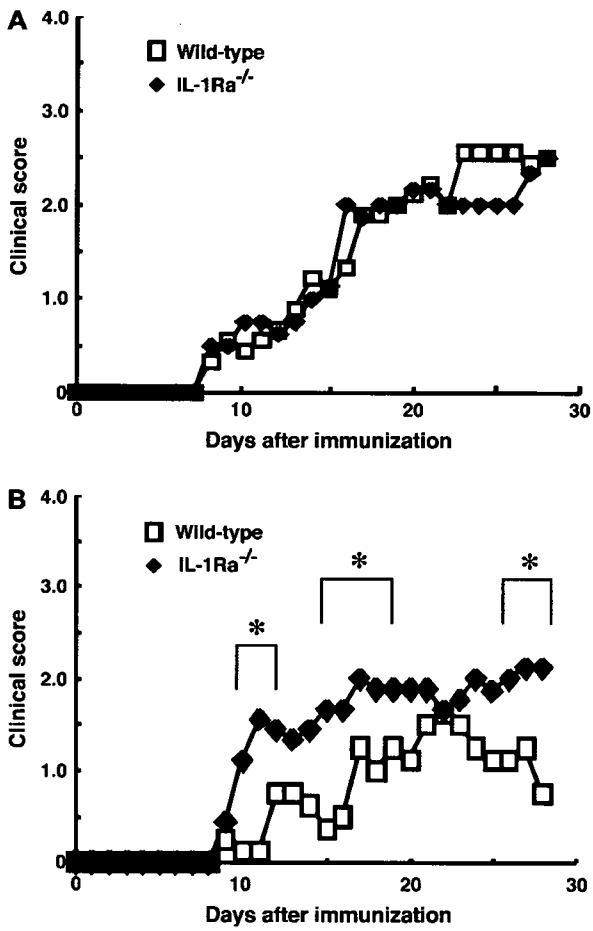

Fig. 2. Exacerbated EAE induction without PTx injection in IL-$1Ra^{-/-}$ mice. Clinical scores after MOG immunization in the (A) presence or (B) absence of PTx (500 ng) injection in wild-type [open squares, (A) $n = 13$ and (B) $n = 8$], and IL-$1Ra^{-/-}$ mice [filled diamonds, (A) $n = 12$ and (B) $n = 9$]. Data show the average from each group. Statistical significances were determined by Mann–Whitney's *U*-test. *$P < 0.05$ versus wild-type mice.

T_h1-type antibody production against MOG 35–55 is increased in sera of IL-$1Ra^{-/-}$ mice

Auto-antigen-specific Igs were detected in the sera of mice with EAE. At 37 days after immunization with MOG 35–55, blood samples were collected from mice for the measurement of MOG-specific auto-antibody levels in the sera. The levels of MOG-specific IgG and IgM classes and the IgG1 subclass in sera, as well as those of IgG2b and IgG3 (data not shown), were comparable among IL-$1^{-/-}$ and wild-type mice given PTx and among IL-$1Ra^{-/-}$ and wild-type mice in the absence of PTx co-administration (Fig. 3A and B). In contrast, the levels of MOG-specific IgG2a, whose production depends on T_h1 cytokines, were significantly increased in sera from IL-$1Ra^{-/-}$ mice in comparison with those from wild-type and IL-$1^{-/-}$ mice (Fig. 3A and B). These results suggest that IL-1 signaling promotes the polarization of T_h1 immune responses toward the production of high levels of auto-antigen-specific IgG2a, as seen in IL-$1Ra^{-/-}$ mice during the development of EAE.

IL-1 is involved in auto-antigen-specific T cell activation during EAE

EAE is considered to be a T cell-mediated autoimmune disease model (3). Abnormal EAE induction in IL-$1^{-/-}$ and IL-$1Ra^{-/-}$ mice may be due to abnormal control of MOG-specific effector T cells. DCs also play a significant role in (auto)immune responses through the induction of T_h1 cell activation (26). In the EAE animal model, we examined if dysfunction of the IL-1/IL-1Ra system affected T cell or DC function using IL-$1^{-/-}$ and IL-$1Ra^{-/-}$ mice. We examined *in vitro* the activation of T cells derived from wild-type, IL-$1^{-/-}$ and IL-$1Ra^{-/-}$ mice immunized with MOG 35–55/CFA in the absence of PTx co-administration. Ten days after MOG 35–55 immunization, $Thy1.2^+$ T cells and $CD11c^+$ DCs were isolated from the draining LNs and spleen, respectively. LN T cells were then co-cultured with DCs in the presence of MOG 35–55. No proliferative responses were observed in DCs of gene-deficient and/or wild-type mice treated with MOG 35–55 in the absence of T cells (data not shown). Low proliferative responses of T cells were observed even without DCs in the absence or presence of MOG 35–55 (data not shown). When cultured with DCs in the presence of MOG 35–55, MOG-specific T cell proliferative responses were induced in a manner dependent on MOG 35–55 concentration (0, 10, 50 and 100 μg ml^{-1}) (data not shown). In these co-cultures, the MOG-specific proliferative responses of wild-type T cells were comparable among wild-type, IL-$1Ra^{-/-}$ and IL-$1^{-/-}$ DCs (Fig. 4A and B), suggesting that IL-1 or IL-1Ra deficiency

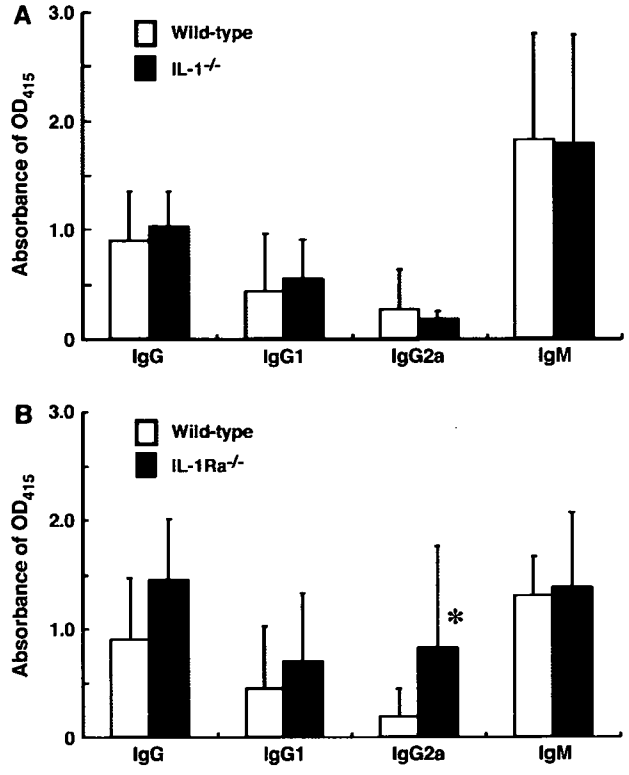

Fig. 3. Titer of anti-MOG antibodies in serum of IL-1$^{-/-}$ and IL-1Ra$^{-/-}$ mice. Thirty-seven days after EAE induction (A) with PTx injection (wild-type, open bars and IL-1$^{-/-}$ mice, filled bars) or (B) without PTx injection (wild-type, open bars and IL-1Ra$^{-/-}$ mice, filled bars), we collected serum samples. The levels of IgG, IgG1, IgG2a and IgM specific for the MOG 35–55 peptide are shown as OD values. Data show the average ± SD from each group. Statistical significances were determined by Student's *t*-test. *$P < 0.05$ versus wild-type mice.

of DCs did not result in any defects in antigen presentation or cytokine production that would influence the induction of MOG-specific T cell recall responses *in vitro*. Interestingly, the proliferative responses of MOG-specific IL-1Ra$^{-/-}$ T cells were significantly hyperactive following co-cultured with either wild-type (Fig. 4D) or IL-1Ra$^{-/-}$ (data not shown) DCs in comparison with wild-type T cells. In contrast, the responses of IL-1$^{-/-}$ T cells after co-culture with either wild-type (Fig. 4C) or IL-1$^{-/-}$ (data not shown) DCs were profoundly impaired, despite comparable non-specific proliferative responses of T cells against mitogenic stimuli Con A 1 μg ml^{-1}) (Fig. 4). These results indicate that intrinsic IL-1 is responsible for the activation of auto-antigen-specific T cells during the priming process *in vivo*.

T cells from IL-1Ra$^{-/-}$ mice produce high levels of pro-inflammatory cytokines

We measured cytokine production by MOG-specific T cells by assaying the supernatants of proliferative response cultures. The levels of IFN-γ and TNFα in supernatants from wild-type T cells co-cultured with either IL-1$^{-/-}$ or IL-1Ra$^{-/-}$ DCs were similar to those cultured with wild-type DCs. In contrast, the levels of IFN-γ and IL-17, but not TNFα, in the supernatants of IL-1$^{-/-}$ T cells co-cultures with wild-type DCs was reduced from the levels seen in wild-type T cells co-cultures with wild-type DCs (Fig. 5A and data not shown). In correlation with MOG-specific T cell proliferative responses, IFN-γ, IL-17 and TNFα levels measured in the supernatants of IL-1Ra$^{-/-}$ T cells co-cultures with wild-type or IL-1Ra$^{-/-}$ DCs were significantly increased in comparison with those from wild-type or IL-1$^{-/-}$ T cells co-cultured with wild-type DCs (Fig. 5B and data not shown). The levels of IL-4, a T_h2-skewing cytokine, were below the limits of detection in the supernatants from any of the culture conditions (data not shown). These results suggest that excess IL-1 signaling breaks tolerance for auto-antigens in peripheral lymphoid tissues, resulting in hyperresponsive effector T cell activation and auto-antigen-specific T cell proliferation and inflammatory cytokine production as seen in IL-1Ra$^{-/-}$ mice during EAE pathogenesis.

Discussion

Using IL-1α$^{-/-}$, IL-1β$^{-/-}$, IL-1$^{-/-}$ and IL-1Ra$^{-/-}$ mice, we demonstrate that IL-1 is responsible for the development of EAE. Either IL-1α or IL-1β alone was sufficient to induce EAE; excess IL-1 signaling resulting from the lack of IL-1Ra augmented EAE severity in the absence of PTx injection. These findings suggested that the adjuvant effect of PTx exerts a related function as IL-1 in the induction of EAE. We clearly demonstrated that, while IL-1 controls optimal antigen-specific T cell activation, dysfunction of the IL-1/IL-1Ra system leads to excess T cell activation by breaking peripheral tolerance for auto-antigens during the pathogenesis of EAE.

In a series of inflammatory response models, we have previously shown that antigen-presenting cell (APC)-derived IL-1 was required for (auto)antigen-specific T cell activation. We previously showed that IL-1 plays an important role in the interaction between T cells and APCs in priming process through inducing CD40L (CD154) and OX40 (CD134) on T cells (25). CD40L and OX40 expressions were enhanced in T cells stimulated with antigen-bearing IL-1Ra$^{-/-}$ APCs compared with wild-type APCs (25). Thus, upon interaction with antigens, APCs produce IL-1, and IL-1 activates T cells, resulting in the induction of CD40L (34, 35). Then, CD40L–CD40 interaction activates APCs to produce TNFα (34). This TNFα induces OX40 on T cells (36), that leads to enhancement of cytokine production, especially IL-17 (37). With these mechanisms, APCs-derived IL-1 contributes to the development of allergic and/or autoimmune diseases in mice (28, 36, 38). IL-1RI$^{-/-}$ DCs demonstrate impaired cytokine production, leading to insufficient CD4$^+$ T cell activation (26). Thus, IL-1 can modulate T cell function both directly and indirectly by influencing DC activation. These findings suggest that IL-1 may play a role in the induction and/or activation of auto-reactive T cells in EAE. Despite comparable non-specific T cell proliferation upon stimulation with mitogen Con A among wild-type, IL-1$^{-/-}$ and IL-1Ra$^{-/-}$ mice (Fig. 4C and D), the proliferation of MOG-specific IL-1$^{-/-}$ T cells co-cultured with wild-type DCs, which can produce IL-1, was markedly impaired. The proliferation of IL-1Ra$^{-/-}$ T cells co-cultured with wild-type DCs, which could produce IL-1Ra, was greatly enhanced (Fig. 4C and D). The proliferation of MOG-specific wild-type T cells co-cultured with IL-1$^{-/-}$ DCs was similar to that observed with wild-type DCs (Fig. 4A), indicating that DC-derived IL-1 is not essential for the activation of MOG-specific

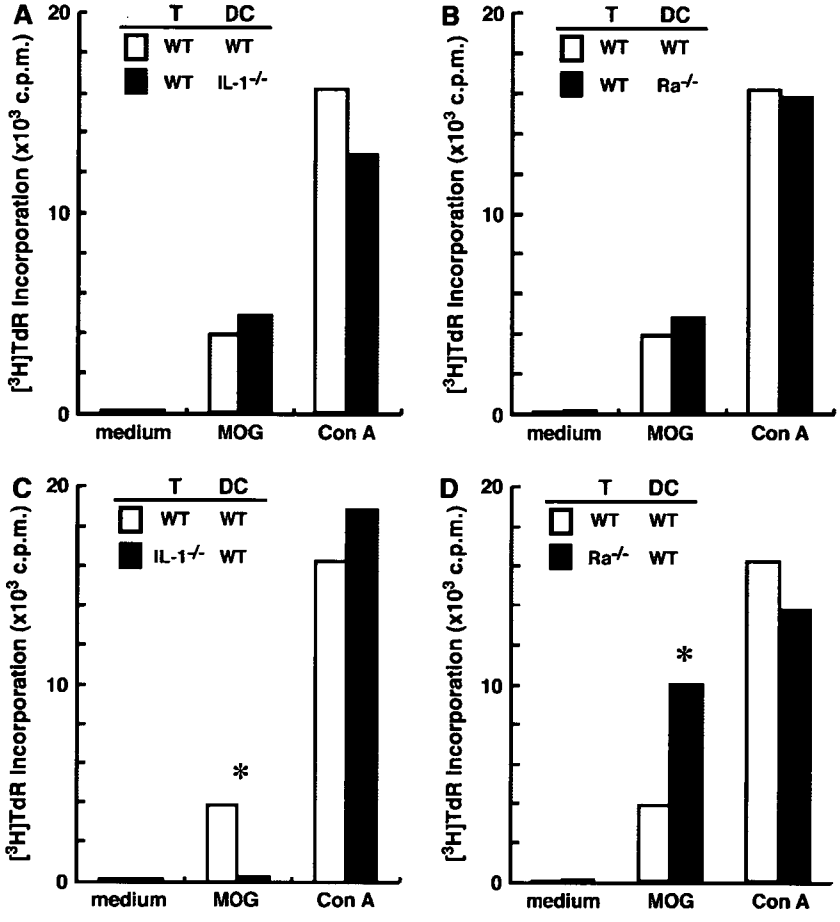

Fig. 4. Abnormal Tcell activation in IL-$1^{-/-}$ and IL-$1Ra^{-/-}$ mice immunized with MOG. Wild-type, IL-$1^{-/-}$ and IL-$1Ra^{-/-}$ mice were immunized with a MOG 35–55/CFA emulsion without PTx co-administration. Ten days after MOG immunization, LN T cells were cultured with splenic DCs in the absence (medium) or presence MOG of MOG 35–55 (100 μg ml^{-1}) or Con A (1 μg ml^{-1}) for 72 h. MOG-sensitized T cells from wild-type mice were co-cultured with DCs from (A) wild-type or IL-$1^{-/-}$ mice and (B) wild-type or IL-$1Ra^{-/-}$ mice. MOG-sensitized T cells from (C) wild-type or IL-$1^{-/-}$ mice and (D) wild-type or IL-$1Ra^{-/-}$ mice were co-cultured with DCs from wild-type mice. The genotypes of the T cells (T) and DCs (DC) are indicated as WT: wild-type mice, IL-$1^{-/-}$: IL-$1^{-/-}$ mice and $Ra^{-/-}$: IL-$1Ra^{-/-}$ mice. Data indicate the averages. These data were reproducible in three independent experiments. Statistical significances were determined by one-way ANOVA and Fisher's protected least significant difference test. *$P < 0.01$ versus wild-type mice.

memory T cells. Instead, IL-1 is likely involved in the induction of MOG-specific memory T cells *in vivo*. Thus, insufficient induction of MOG-specific T cells resulting from IL-1 deficiency may lead to the attenuated development of EAE as observed in IL-$1^{-/-}$ mice. In contrast, excess MOG-specific T cell activation observed in IL-1Ra-deficient mice may explain the exacerbation of EAE in IL-$1Ra^{-/-}$ mice.

Despite the normal development of EAE following PTx injection, IL-$1Ra^{-/-}$ mice exhibited more severe MOG-induced EAE in the absence of PTx injection than wild-type mice. Similarly, the development of EAE in TNFα$^{-/-}$ mice was completely suppressed in the presence of low doses of PTx, although susceptibility to the disease in TNFα$^{-/-}$ mice was normal at high doses of PTx (33). PTx is widely used to enhance T_h1-mediated organ-specific autoimmune disease through inhibition of the Gi/o protein signaling pathways that negatively regulate IL-12 production (39) and induction of pro-inflammatory cytokines, MHC class II, CD80, CD86 and CD40 on APCs (40, 41). These observations imply that PTx exerts a similar function as the pro-inflammatory cytokines IL-1 and TNFα. We, as well as others, previously observed that the function of IL-1 in ovalbumin-induced airway hypersensitivity responses could be substituted for by a potent adjuvant, aluminum potassium sulfate (42, 43). Therefore, the physiological function of IL-1 (and TNFα) may be masked by the excessive adjuvant-dependent artificial activation of the immune system observed in MOG–EAE with PTx injection and ovalbumin-induced airway hypersensitivity responses with aluminum potassium sulfate.

IFN-γ, TNFα and IL-17, T cell-derived inflammatory cytokines, play critical roles in multiple pathological inflammatory responses. TNFα has a similar biological activity to IL-1 as a potent pro-inflammatory cytokine. As seen in studies using TNFα$^{-/-}$ mice, TNFα is also involved in the development of EAE (13, 14). Interestingly, TNFα production is normal in IL-$1^{-/-}$ mice after MOG/CFA immunization (Fig. 5A), despite the profound suppression of EAE development in IL-$1^{-/-}$ mice (Fig. 1 and Table 1). In contrast, IL-$1Ra^{-/-}$ mice exhibited elevated TNFα production (Fig. 5B) and exacerbated development of EAE (Fig. 2 and Table 1). Thus, TNFα is not essential for, but contributes to, the development of EAE (15, 23, 44). Excess TNFα production resulting from excessive

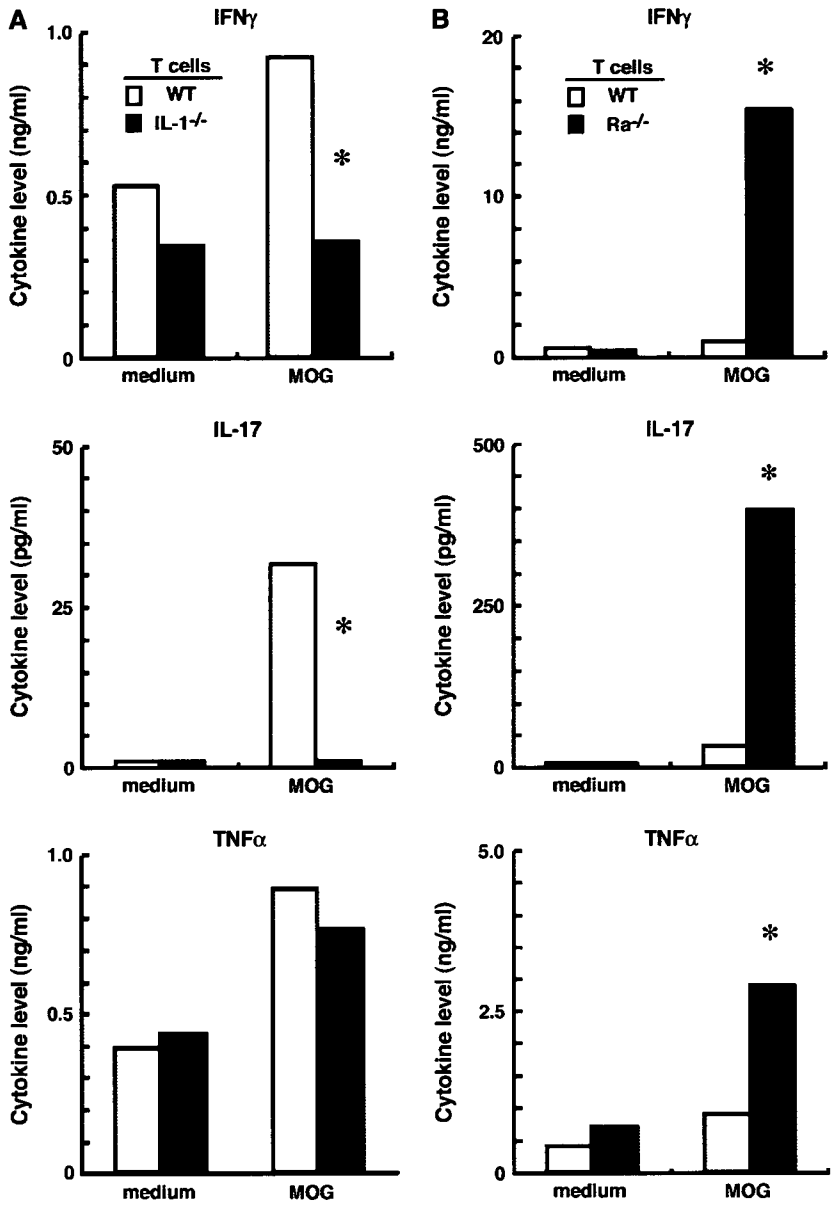

Fig. 5. Abnormal cytokine production from IL-$1^{-/-}$ T cells and IL-$1Ra^{-/-}$ T cells. MOG-sensitized T cells from (A) wild-type or IL-$1^{-/-}$ mice and (B) wild-type or IL-$1Ra^{-/-}$ mice were co-cultured with wild-type DCs in the absence (medium) or presence MOG of MOG 35–55, as shown in Fig. 4. IFN-γ, IL-17 and TNFα levels in culture supernatants were determined by ELISA. The genotypes of the T cells are indicated as WT: wild-type mice, IL-$1^{-/-}$: IL-$1^{-/-}$ mice and $Ra^{-/-}$: IL-$1Ra^{-/-}$ mice. Data indicate the averages. These data were reproducible in two independent experiments. Statistical significances were determined by one-way ANOVA and Fisher's protected least significant difference test. *$P < 0.01$ versus wild-type mice.

IL-1 activity may explain the synergistic exacerbation of EAE development in IL-$1Ra^{-/-}$ mice. These results suggest, however, that TNFα alone is not sufficient to induce adequate responses in the absence of IL-1, as observed in IL-$1^{-/-}$ mice.

While IFN-γ-producing T_h1 cells are crucial for the induction of autoimmune diseases, IFN-$\gamma^{-/-}$ and/or IFN-$\gamma R^{-/-}$ mice develop autoimmune diseases, such as EAE and collagen-induced arthritis (6–9, 45). Currently, T cell-derived IL-17, rather than IFN-γ, is suspected to be critical in the pathogenesis of EAE. In support of this hypothesis, increased levels of IL-17 were observed in the lesions of MS patients (46). Otherwise, IL-12 has been well characterized as a potent activator of IFN-γ-producing T_h1 cells, while IL-23, a member of the IL-12 family consisting of IL-23 p19 and IL-12 p40, can induce IL-17 production by T cells (47). IL-23, but not IL-12, is crucial for the development of EAE (48). As seen with IFN-$\gamma^{-/-}$ and IL-$12^{-/-}$ mice, IL-12Rβ$2^{-/-}$ mice exhibited exacerbated EAE development and increased IL-17 production (49). IL-12 administration, however, led to the inhibition of IL-17 mRNA expression during EAE pathogenesis (50). Currently, the contribution of IL-17 to the pathogenesis of EAE was suggested in mice treated with anti-IL-17-neutralizing antibody (51). We

determined that, in MOG-stimulated T cells, IL-17 production was reduced in IL-$1^{-/-}$ mice and increased in IL-$1Ra^{-/-}$ mice (Fig. 5A and B). Thus, our data suggest that IL-1 plays an important role in the activation of both IFN-γ-producing T_h1 and IL-17-producing $CD4^+$ T cells, contributing to the development of EAE.

In conclusion, our findings suggest that dysregulation of the IL-1/IL-1Ra balance leads to the failure of peripheral lymphoid tolerance for self-antigens, resulting in the severe inflammation seen in EAE. These observations may provide a clue to develop new therapeutics against MS.

Acknowledgements

We would like to thank Ohmi for providing the MOG peptide. We would also like to thank K. Habu and Y. Komiyama for their technical support and critical comments. We thank all the members of our laboratory for their kind discussion and help in animal care. This work was supported by grants from the Ministry of Education, Science, Sport and Culture of Japan, the Ministry of Health and Welfare of Japan, the Japan Society for the Promotion of Science and Pioneering Research Project in Biotechnology.

Abbreviations

ANOVA	analysis of variance
APC	antigen-presenting cell
CNS	central nervous system
DC	dendritic cell
EAE	experimental autoimmune encephalomyelitis
IL-1Ra	IL-1R antagonist
IL-1RI	IL-1R type-I
LN	lymph node
MOG	myelin oligodendrocyte glycoprotein
MS	multiple sclerosis
PTx	pertussis toxin
[^{3}H]TdR	[^{3}H]thymidine
TNF	tumor necrosis factor

References

1 Steinman, L., Martin, R., Bernard, C., Conlon, P. and Oksenberg, J. R. 2002. Multiple sclerosis: deeper understanding of its pathogenesis reveals new targets for therapy. *Annu. Rev. Neurosci.* 25:491.
2 Keegan, B. M. and Noseworthy, J. H. 2002. Multiple sclerosis. *Annu. Rev. Med.* 53:285.
3 Kuchroo, V. K., Anderson, A. C., Waldner, H., Munder, M., Bettelli, E. and Nicholson, L. B. 2002. T cell response in experimental autoimmune encephalomyelitis (EAE): role of self and cross-reactive antigens in shaping, tuning, and regulating the autopathogenic T cell repertoire. *Annu. Rev. Immunol.* 20:101.
4 Hemmer, B., Archelos, J. J. and Hartung, H. P. 2002. New concepts in the immunopathogenesis of multiple sclerosis. *Nat. Rev. Neurosci.* 3:291.
5 Owens, T., Wekerle, H. and Antel, J. 2001. Genetic models for CNS inflammation. *Nat. Med.* 7:161.
6 Ferber, I. A., Brocke, S., Taylor-Edwards, C. *et al.* 1996. Mice with a disrupted IFN-γ gene are susceptible to the induction of experimental autoimmune encephalomyelitis (EAE). *J. Immunol.* 156:5.
7 Krakowski, M. and Owens, T. 1996. Interferon-γ confers resistance to experimental allergic encephalomyelitis. *Eur. J. Immunol.* 26: 1641.
8 Willenborg, D. O., Fordham, S., Bernard, C. C., Cowden, W. B. and Ramshaw, I. A. 1996. IFN-γ plays a critical down-regulatory role in the induction and effector phase of myelin oligodendrocyte glycoprotein-induced autoimmune encephalomyelitis. *J. Immunol.* 157:3223.
9 Chu, C. Q., Wittmer, S. and Dalton, D. K. 2000. Failure to suppress the expansion of the activated CD4 T cell population in interferon γ-deficient mice leads to exacerbation of experimental autoimmune encephalomyelitis. *J. Exp. Med.* 192:123.
10 Furlan, R., Brambilla, E., Ruffini, F. *et al.* 2001. Intrathecal delivery of IFN-γ protects C57BL/6 mice from chronic-progressive experimental autoimmune encephalomyelitis by increasing apoptosis of central nervous system-infiltrating lymphocytes. *J. Immunol.* 167: 1821.
11 Probert, L., Akassoglou, K., Pasparakis, M., Kontogeorgos, G. and Kollias, G. 1995. Spontaneous inflammatory demyelinating disease in transgenic mice showing central nervous system-specific expression of tumor necrosis factor α. *Proc. Natl Acad. Sci. USA* 92:11294.
12 Powell, M. B., Mitchell, D., Lederman, J. *et al.* 1990. Lymphotoxin and tumor necrosis factor-α production by myelin basic protein-specific T cell clones correlates with encephalitogenicity. *Int. Immunol.* 2:539.
13 Sedgwick, J. D., Riminton, D. S., Cyster, J. G. and Korner, H. 2000. Tumor necrosis factor: a master-regulator of leukocyte movement. *Immunol. Today* 21:110.
14 Sean Riminton, D., Korner, H., Strickland, D. H., Lemckert, F. A., Pollard, J. D. and Sedgwick, J. D. 1998. Challenging cytokine redundancy: inflammatory cell movement and clinical course of experimental autoimmune encephalomyelitis are normal in lymphotoxin-deficient, but not tumor necrosis factor-deficient, mice. *J. Exp. Med.* 187:1517.
15 Kassiotis, G. and Kollias, G. 2001. Uncoupling the proinflammatory from the immunosuppressive properties of tumor necrosis factor (TNF) at the p55 TNF receptor level: implications for pathogenesis and therapy of autoimmune demyelination. *J. Exp. Med.* 193:427.
16 Kollias, G. and Kontoyiannis, D. 2002. Role of TNF/TNFR in autoimmunity: specific TNF receptor blockade may be advantageous to anti-TNF treatments. *Cytokine Growth Factor Rev.* 13:315.
17 Tocci, M. J. and Schmidt, J. A. 1997. Interleukin-1: structure and function. In Remick, D. G. and Friedland, J. S., eds, *Cytokines in Health and Disease*, 2nd edn, p. 1. Dekker Encyclopedias, Taylor and Francis Group, KY, USA.
18 Tamaru, M., Tomura, K., Sakamoto, S., Tezuka, K., Tamatani, T. and Narumi, S. 1998. Interleukin-1β induces tissue- and cell type-specific expression of adhesion molecules *in vivo*. *Arterioscler. Thromb. Vasc. Biol.* 18:1292.
19 Horai, R., Saijo, S., Tanioka, H. *et al.* 2000. Development of chronic inflammatory arthropathy resembling rheumatoid arthritis in interleukin 1 receptor antagonist-deficient mice. *J. Exp. Med.* 191:313.
20 Nicklin, M. J., Hughes, D. E., Barton, J. L., Ure, J. M. and Duff, G. W. 2000. Arterial inflammation in mice lacking the interleukin 1 receptor antagonist gene. *J. Exp. Med.* 191:303.
21 Jacobs, C. A., Baker, P. E., Roux, E. R. *et al.* 1991. Experimental autoimmune encephalomyelitis is exacerbated by IL-1α and suppressed by soluble IL-1 receptor. *J. Immunol.* 146:2983.
22 Martin, D. and Near, S. L. 1995. Protective effect of the interleukin-1 receptor antagonist (IL-1ra) on experimental allergic encephalomyelitis in rats. *J. Neuroimmunol.* 61:241.
23 Schiffenbauer, J., Streit, W. J., Butfiloski, E., LaBow, M., Edwards, C., III and Moldawer, L. L. 2000. The induction of EAE is only partially dependent on TNF receptor signaling but requires the IL-1 type I receptor. *Clin. Immunol.* 95:117.
24 Mannie, M. D., Dinarello, C. A. and Paterson, P. Y. 1987. Interleukin 1 and myelin basic protein synergistically augment adoptive transfer activity of lymphocytes mediating experimental autoimmune encephalomyelitis in Lewis rats. *J. Immunol.* 138:4229.
25 Nakae, S., Asano, M., Horai, R., Sakaguchi, N. and Iwakura, Y. 2001. IL-1 enhances T cell-dependent antibody production through induction of CD40 ligand and OX40 on T cells. *J. Immunol.* 167:90.
26 Eriksson, U., Kurrer, M. O., Sonderegger, I. *et al.* 2003. Activation of dendritic cells through the interleukin 1 receptor 1 is critical for the induction of autoimmune myocarditis. *J. Exp. Med.* 197:323.
27 Shornick, L. P., Bisarya, A. K. and Chaplin, D. D. 2001. IL-1β is essential for langerhans cell activation and antigen delivery to the

lymph nodes during contact sensitization: evidence for a dermal source of IL-1β. *Cell. Immunol.* 211:105.
28 Nakae, S., Naruse-Nakajima, C., Sudo, K., Horai, R., Asano, M. and Iwakura, Y. 2001. IL-1α, but not IL-1β, is required for contact-allergen-specific T cell activation during the sensitization phase in contact hypersensitivity. *Int. Immunol.* 13:1471.
29 Horai, R., Asano, M., Sudo, K. *et al.* 1998. Production of mice deficient in genes for interleukin (IL)-1α, IL-1β, IL-1α/β, and IL-1 receptor antagonist shows that IL-1β is crucial in turpentine-induced fever development and glucocorticoid secretion. *J. Exp. Med.* 187:1463.
30 Nakae, S., Asano, M., Horai, R. and Iwakura, Y. 2001. Interleukin-1β, but not interleukin-1α, is required for T-cell-dependent antibody production. *Immunology* 104:402.
31 Nakae, S., Komiyama, Y., Nambu, A. *et al.* 2002. Antigen-specific T cell sensitization is impaired in IL-17-deficient mice, causing suppression of allergic cellular and humoral responses. *Immunity* 17:375.
32 Bettelli, E., Das, M. P., Howard, E. D., Weiner, H. L., Sobel, R. A. and Kuchroo, V. K. 1998. IL-10 is critical in the regulation of autoimmune encephalomyelitis as demonstrated by studies of IL-10- and IL-4-deficient and transgenic mice. *J. Immunol.* 161: 3299.
33 Kassiotis, G., Kranidioti, K. and Kollias, G. 2001. Defective CD4T cell priming and resistance to experimental autoimmune encephalomyelitis in TNF-deficient mice due to innate immune hyporesponsiveness. *J. Neuroimmunol.* 119:239.
34 van Kooten, C. and Banchereau, J. 2000. CD40-CD40 ligand. *J. Leukoc. Biol.* 67:2.
35 Weinberg, A. D., Bourdette, D. N., Sullivan, T. J. *et al.* 1996. Selective depletion of myelin-reactive T cells with the anti-OX-40 antibody ameliorates autoimmune encephalomyelitis. *Nat. Med.* 2:183.
36 Horai, R., Nakajima, A., Habiro, K. *et al.* 2004. TNF-α is crucial for the development of autoimmune arthritis in IL-1 receptor antagonist-deficient mice. *J. Clin. Investig.* 114:1603.
37 Nakae, S., Saijo, S., Horai, R., Sudo, K., Mori, S. and Iwakura, Y. 2003. IL-17 production from activated T cells is required for the spontaneous development of destructive arthritis in mice deficient in IL-1 receptor antagonist. *Proc. Natl Acad. Sci. USA* 100:5986.
38 Saijo, S., Asano, M., Horai, R., Yamamoto, H. and Iwakura, Y. 2002. Suppression of autoimmune arthritis in interleukin-1-deficient mice in which T cell activation is impaired due to low levels of CD40 ligand and OX40 expression on T cells. *Arthritis Rheum.* 46:533.
39 He, J., Gurunathan, S., Iwasaki, A., Ash-Shaheed, B. and Kelsall, B. L. 2000. Primary role for Gi protein signaling in the regulation of interleukin 12 production and the induction of T helper cell type 1 responses. *J. Exp. Med.* 191:1605.
40 Shive, C. L., Hofstetter, H., Arredondo, L., Shaw, C. and Forsthuber, T. G. 2000. The enhanced antigen-specific production of cytokines induced by pertussis toxin is due to clonal expansion of T cells and not to altered effector functions of long-term memory cells. *Eur. J. Immunol.* 30:2422.
41 Ryan, M., McCarthy, L., Rappuoli, R., Mahon, B. P. and Mills, K. H. 1998. Pertussis toxin potentiates Th1 and Th2 responses to co-injected antigen: adjuvant action is associated with enhanced regulatory cytokine production and expression of the co-stimulatory molecules B7-1, B7-2 and CD28. *Int. Immunol.* 10:651.
42 Nakae, S., Komiyama, Y., Yokoyama, H. *et al.* 2003. IL-1 is required for allergen-specific Th2 cell activation and the development of airway hypersensitivity response. *Int. Immunol.* 15:483.
43 Schmitz, N., Kurrer, M. and Kopf, M. 2003. The IL-1 receptor 1 is critical for Th2 cell type airway immune responses in a mild but not in a more severe asthma model. *Eur. J. Immunol.* 33:991.
44 Frei, K., Eugster, H. P., Bopst, M., Constantinescu, C. S., Lavi, E. and Fontana, A. 1997. Tumor necrosis factor α and lymphotoxin α are not required for induction of acute experimental autoimmune encephalomyelitis. *J. Exp. Med.* 185:2177.
45 Manoury-Schwartz, B., Chiocchia, G., Bessis, N. *et al.* 1997. High susceptibility to collagen-induced arthritis in mice lacking IFN-γ receptors. *J. Immunol.* 158:5501.
46 Lock, C., Hermans, G., Pedotti, R. *et al.* 2002. Gene-microarray analysis of multiple sclerosis lesions yields new targets validated in autoimmune encephalomyelitis. *Nat. Med.* 8:500.
47 Aggarwal, S., Ghilardi, N., Xie, M. H., de Sauvage, F. J. and Gurney, A. L. 2003. Interleukin-23 promotes a distinct CD4 T cell activation state characterized by the production of interleukin-17. *J. Biol. Chem.* 278:1910.
48 Cua, D. J., Sherlock, J., Chen, Y. *et al.* 2003. Interleukin-23 rather than interleukin-12 is the critical cytokine for autoimmune inflammation of the brain. *Nature* 421:744.
49 Zhang, G. X., Gran, B., Yu, S. *et al.* 2003. Induction of experimental autoimmune encephalomyelitis in IL-12 receptor-β2-deficient mice: IL-12 responsiveness is not required in the pathogenesis of inflammatory demyelination in the central nervous system. *J. Immunol.* 170:2153.
50 Gran, B., Chu, N., Zhang, G. X. *et al.* 2004. Early administration of IL-12 suppresses EAE through induction of interferon-γ. *J. Neuroimmunol.* 156:123.
51 Langrish, C. L., Chen, Y., Blumenschein, W. M. *et al.* 2005. IL-23 drives a pathogenic T cell population that induces autoimmune inflammation. *J. Exp. Med.* 201:233.

Development/Plasticity/Repair

Mammalian Motoneuron Axon Targeting Requires Receptor Protein Tyrosine Phosphatases σ and δ

Noriko Uetani,[1] Mélanie J. Chagnon,[1] Timothy E. Kennedy,[2] Yoichiro Iwakura,[3] and Michel L. Tremblay[1]

[1]McGill Cancer Centre and Department of Biochemistry, McGill University, Montreal, Quebec, Canada H3G 1Y6, [2]Centre for Neuronal Survival, Department of Neurology and Neurosurgery, Montreal Neurological Institute, McGill University, Montreal, Quebec, Canada H3A 2B4, and [3]Center for Experimental Medicine, Institute of Medical Sciences, University of Tokyo, Tokyo 108-8639, Japan

The leukocyte common antigen-related (LAR) subfamily of receptor protein tyrosine phosphatases (RPTPs), LAR, RPTP-σ, and RPTP-δ, regulate neuroendocrine development, axonal regeneration, and hippocampal long-term potentiation in mammals. In *Drosophila*, RPTPs are required for appropriate axon targeting during embryonic development. In contrast, deletion of any one of the three LAR-RPTP family members in mammals does not result in gross axon targeting defects. Both RPTP-σ and RPTP-δ are highly expressed in the developing mammalian nervous system, suggesting they might be functionally redundant. To test this hypothesis, we generated RPTP-σ and RPTP-δ (RPTP-σ/δ) double-mutant mice. Although embryonic day 18.5 RPTP-σ and RPTP-δ single-mutant embryos were viable, RPTP-σ/δ double mutants were paralyzed, were never observed to draw a breath, and died shortly after cesarean section. RPTP-σ/δ double mutants exhibit severe muscle dysgenesis and severe loss of motoneurons in the spinal cord. Detailed analysis of the projections of phrenic nerves in RPTP-σ/δ double mutants indicated that these motoneuron axons emerge normally from the cervical spinal cord, but stall on reaching the diaphragm. Our results demonstrate that RPTP-σ and RPTP-δ complement each other functionally during mammalian development, and reveal an essential contribution of RPTP-σ and RPTP-δ to appropriate motoneuron axon targeting during mammalian axonogenesis.

Key words: protein tyrosine phosphatase; tyrosine phosphorylation; axon targeting; axon guidance; motoneuron (motor neuron); phrenic; σ; δ

Introduction

Receptor protein tyrosine phosphatases (RPTPs) are key regulators of axon guidance in *Drosophila* (Johnson and Van Vactor, 2003). For example, loss-of-function mutants of leukocyte common antigen-related (LAR) subfamily RPTPs [*Drosophila* LAR (DLAR)] exhibit defects in motor axon guidance, midline axon crossing, and photoreceptor axon guidance (Desai et al., 1996; Krueger et al., 1996; Sun et al., 2000; Clandinin et al., 2001; Maurel-Zaffran et al., 2001; Desai and Purdy, 2003). There are three vertebrate homologs of DLAR: PTPRS (RPTP-σ), PTPRD (RPTP-δ), and PTPRF (LAR) (Johnson and Holt, 2000; Johnson and Van Vactor, 2003).

Received June 27, 2005; revised April 18, 2006; accepted April 19, 2006.

This work was supported by funding from the Canadian Institutes of Health Research (CIHR) (MOP-42482 to M.L.T.). M.L.T. is a Chercheur National du Fonds de la Recherche en Santé du Québec (FRSQ) and a holder of the Jeanne and Jean-Louis Levesque Chair in Cancer Research. T.E.K. holds a FRSQ Chercheur-Boursier award. N.U. is a recipient of a CIHR-funded Chemical Biology Postgraduate Training award. M.J.C. is a recipient of a FRSQ Doctoral Training Award. We thank Eva Migon and Lisa Michelle Read for their help with excellent animal care, and Cortney Trott for genotyping mice. We also thank all members of the Tremblay laboratory for their valuable discussions. The monoclonal antibodies against Islet-1/2 (39.4D5) developed by Dr. Thomas M. Jessell and neurofilament (2H3) developed by Drs. Thomas M. Jessell and Jane Dodd were obtained from the Developmental Studies Hybridoma Bank developed under the auspices of the National Institute of Child Health and Human Development and maintained by the Department of Biological Sciences, University of Iowa (Iowa City, IA).

Correspondence should be addressed to Michel L. Tremblay, McGill Cancer Centre, McIntyre Medical Sciences Building, McGill University, 3655 Promenade Sir-William-Osler, Room 701, Montreal, Quebec, Canada H3G 1Y6. E-mail: michel.tremblay@mcgill.ca.

DOI: 10.1523/JNEUROSCI.0386-06.2006

 0270-6474/06/265872-09$15.00/0

Type IIa RPTPs are characterized by variable numbers of extracellular Ig-like and type-III fibronectin (FNIII) repeats and two intracellular tandem phosphatase domains. The extracellular domains of this family resemble cell adhesion molecules (CAMs), suggesting that they play roles in cell–cell and cell–matrix interactions (Brady-Kalnay and Tonks, 1995; Beltran and Bixby, 2003).

In vertebrates, type IIa RPTPs are present in axons and growth cones (Tian et al., 1991; Desai et al., 1994; Stoker et al., 1995; Sommer et al., 1997; Schaapveld et al., 1998; Thompson et al., 2003). Although RNA interference-mediated knock-down has provided evidence that they contribute to motor axon guidance in chick (Stepanek et al., 2005), a role for LAR subfamily members in axon guidance during mammalian development has not been reported. Limited levels of LAR expression in the CNS are detected during development, and its absence results in minor defects in cholinergic innervation of the hippocampal dentate gyrus (Yeo et al., 1997; Van Lieshout et al., 2001). In contrast, RPTP-σ and RPTP-δ are highly expressed in the developing mammalian nervous system (Yan et al., 1993; Mizuno et al., 1994; Sommer et al., 1997; Schaapveld et al., 1998). RPTP-σ-deficient mice exhibit abnormal development of the pituitary and neurological defects that include spastic movements and abnormal limb flexion (Elchebly et al., 1999; Wallace et al., 1999). Additionally, the absence of RPTP-σ results in enhanced axon regeneration in both the peripheral and central nervous systems (McLean

et al., 2002; Thompson et al., 2003; Saphieha et al., 2005). Mutant mice lacking an essential catalytic domain of RPTP-δ exhibit early growth retardation and neonatal mortality. In this case, the high mortality is likely attributable to insufficient food intake caused by motor dysfunction. RPTP-δ-deficient mice that reach adulthood show enhanced hippocampal long-term potentiation and impaired spatial learning ability (Uetani et al., 2000).

The overlapping expression patterns of RPTP-σ and RPTP-δ suggest that the phenotypes observed in single gene knock-outs may underestimate the contribution of type IIa RPTPs to mammalian neural development. Consistent with this, RNA interference knock-down suggested overlapping functions for LAR-RPTPs in cultured rat hippocampal neurons (Dunah et al., 2005). To address the possibility of functional redundancy *in vivo*, mice deficient for both RPTP-σ and RPTP-δ were generated and characterized. Our findings demonstrate that RPTP-σ and RPTP-δ are essential for the appropriate innervation of muscles by motoneurons during development of the murine peripheral nervous system.

Materials and Methods

Generation of RPTP-σ/δ double-mutant mice. Mutant mice lacking either RPTP-σ or RPTP-δ have been described previously (Elchebly et al., 1999; Uetani et al., 2000). These animals were backcrossed for at least six generations to C57BL/6J. Double homozygous mutant mice were obtained by intercrossing double heterozygous parents. Noon on the day of the detection of the vaginal plug was considered embryonic day 0.5 (E0.5). To genotype RPTP-σ and RPTP-δ alleles, tissue lysates from mice were used for PCR analysis with allele-specific primers: Sigma-WT-R2, 5′-TAG TCA GAG CCC TCC ACA CCG-3′; Sigma-KO-F1, 5′-CAG CGA CCT CCA ACA CAC AAG-3′; Sigma-WT-F2, 5′-CAT TTC CAG TTC ACG GCA TGG C-3′; Delta-WT-R1, 5′-CTG GAA TTG TCT CAC TTT CCT C-3′; Delta-WT-F1, 5′-CCA GCA GAG GCA CAG AAA CTC-3′; Delta-PGK#5, 5′-GAC TGC CTT GGG AAA AGC GCC TCC-3′.

RPTP-σ wild-type and knock-out alleles are predicted to produce 781 and 1000 bp PCR products, respectively. RPTP-δ wild-type and knock-out alleles are predicted to produce 620 and 380 bp bands, respectively. Amplified bands were the expected size. Mice were kept under specific pathogen-free conditions in an environmentally controlled clean room at the Animal Resource Center of McGill University. All experiments were conducted according to the Canadian Council of Animal Care ethical guidelines for animal experiments.

Animals identified as "control" in this study include littermates with the following genotypes (RPTP-$\sigma^{+/+}/\delta^{+/+}$, RPTP-$\sigma^{+/-}/\delta^{+/+}$, RPTP-$\sigma^{+/+}/\delta^{+/-}$, RPTP-$\sigma^{+/-}/\delta^{+/-}$) with all presenting identical normal (wild-type) phenotypes. Hence they were tabulated together for statistical analysis.

Histological analysis. Tissues were dissected and fixed in phosphate buffered 4% paraformaldehyde (PFA), left overnight in the same fixative, and then embedded in paraffin wax according to standard procedure. Serial 6 μm paraffin sections were made and stained with hematoxylin and eosin (H&E) or cresyl violet (Nissl stain). For every fourth section at the forelimb level (E18.5), the thickness of the dorsal epidermis and dermis was measured at three locations using AxioVision, version 4.0, software (Carl Zeiss, Oberkochen, Germany). The thickness of the diaphragm was measured on E16.5 sagittal sections at eye level in the same way. A total of three sections from each animal was measured and the mean value of these measurements was used as a single data value for statistical analysis by Student's *t* test. Skeletal muscle was visualized in paraffin sections using an antibody against myosin heavy chain (MY32; Sigma, St. Louis, MO; 1:100 dilution; a biotinylated anti-mouse secondary antibody and peroxidase-labeled streptavidin; LSAB kit; DakoCytomation, Carpinteria, CA). The color reaction was developed using 3-3′-diaminobenzidine tetrahydrochloride (DAB) as a chromogen (SigmaFast DAB tablets; Sigma). Histological analyses were performed on E16.5 RPTP-σ/δ double mutants ($n = 2$) with control littermates ($n = 2$), and on E18.5 RPTP-σ/δ double mutants ($n = 3$) with their control littermates ($n = 3$), RPTP-$\sigma^{-/-}/\delta^{+/+}$ ($n = 2$), RPTP-$\sigma^{+/+}/\delta^{-/-}$ ($n = 2$), RPTP-$\sigma^{+/-}/\delta^{-/-}$ ($n = 2$), and RPTP-$\sigma^{-/-}/\delta^{+/-}$ ($n = 2$).

Quantification of motor neurons. E13 and E18.5 embryos were fixed in 4% PFA overnight. Whole E13 embryos were embedded in OCT compound (TissueTek; Sakura Finetek, Torrance, CA). Cervical spinal cords (C3–C5) were dissected from E18.5 embryos and embedded in paraffin. Ten micrometer serial cryostat and paraffin sections were prepared. The location of C3–C5 at E13 was determined morphologically based on surrounding tissue. Mouse anti-Islet-1/2 antibodies (39.4D5; Developmental Studies Hybridoma Bank, Iowa City, IA; supernatant, 1:50 dilution) and goat anti-choline acetyltransferase (ChAT) antibodies (Chemicon, Temecula, CA; 1:100 dilution) were used to identify motoneurons in the E13 and E18.5 spinal cords, respectively. Sections were visualized using secondary antibodies coupled to Alexa 488 (Invitrogen, San Diego, CA), and photographed using a Zeiss Axioskop2 Plus microscope.

Islet-1/2- and ChAT-immunopositive motoneurons were counted independently on right and left hemiventral columns in every fourth section. A total of 10 hemiventral columns from each animal were counted, and the mean value of these counts was used as an individual data point for statistical analysis by Student's *t* test. At E13, RPTP-σ/δ double mutants ($n = 3$) were analyzed with their control ($n = 5$) littermates. At E18.5, RPTP-σ/δ double mutants ($n = 3$) were analyzed with their littermates RPTP-$\sigma^{+/+}/\delta^{+/+}$ ($n = 4$), RPTP-$\sigma^{+/+}/\delta^{-/-}$ ($n = 3$), RPTP-$\sigma^{-/-}/\delta^{+/+}$ ($n = 2$), RPTP-$\sigma^{+/-}/\delta^{-/-}$ ($n = 2$), and RPTP-$\sigma^{-/-}/\delta^{+/-}$ ($n = 4$).

Whole-mount diaphragm staining. To visualize peripheral nerves, whole E12 embryos and thoracic cages dissected from E13.5 and E15.5 embryos were fixed in methanol/dimethylsulfoxide (DMSO) (4:1) at 4°C overnight. Tissues were then immersed in methanol/DMSO/H_2O_2 (4:1:1) at room temperature for 5–10 h to block endogenous peroxidase activity, and rehydrated in 50% methanol and PBS. E12 embryos were embedded in OCT compound, and sagittal sections were cut with a cryostat until heart and liver were visible. The remaining E12 embryonic tissue was immersed in PBS to remove excess OCT and then blocked in PBS containing 5% skimmed milk, 0.5% Triton X-100 (PBSMT). The embryos were incubated in 2 ml of PBSMT with the 2H3 monoclonal antibody against neurofilament (ascites; 1:2000 dilution; 4°C overnight; Developmental Studies Hybridoma Bank) (Dodd et al., 1988). After washing with 4 ml of PBSMT for 1 h at room temperature three times, the embryos were incubated with horseradish peroxidase-conjugated anti-mouse IgG (1:10,000 dilution) (Jackson ImmunoResearch, West Grove, PA) in PBSMT overnight at 4°C. They were then washed with 4 ml of PBSMT for 1 h at room temperature six times, and thoracic cages were soaked in DAB substrate solution to develop the color reaction (SigmaFast DAB tablets; Sigma). Stained diaphragms were dissected from E13.5 and E15.5 thoracic cages in PBS, and dehydrated in an ethanol series. After xylene substitution, diaphragms were mounted on slides. Stained E12 embryos were then dehydrated in methanol and substituted in benzyl alcohol (Sigma) and benzyl benzonate (Sigma) (1:2). Stained diaphragms were photographed and branch points on the sternocostal phrenic nerve were counted using AxioVision, version 4.0, software. E12 RPTP-σ/δ double mutants ($n = 3$) were analyzed with control ($n = 4$) littermates. E13.5 RPTP-σ/δ double mutants ($n = 2$) were analyzed with control ($n = 2$), RPTP-$\sigma^{-/-}/\delta^{+/+}$ ($n = 2$), RPTP-$\sigma^{+/+}/\delta^{-/-}$ ($n = 3$), RPTP-$\sigma^{-/-}/\delta^{+/-}$ ($n = 1$), and RPTP-$\sigma^{+/-}/\delta^{-/-}$ ($n = 2$) littermates. E15.5 RPTP-σ/δ double mutants ($n = 2$) were analyzed with control ($n = 3$), RPTP-$\sigma^{-/-}/\delta^{+/+}$ ($n = 3$), RPTP-$\sigma^{+/+}/\delta^{-/-}$ ($n = 2$), RPTP-$\sigma^{-/-}/\delta^{+/-}$ ($n = 2$), and RPTP-$\sigma^{+/-}/\delta^{-/-}$ ($n = 3$) littermates.

Results

RPTPσ/δ double-mutant mice die at birth

RPTP-σ and RPTP-δ (RPTP-σ/δ) double-mutant mice were generated by breeding adults heterozygous for both RPTP-σ and RPTP-δ (RPTP-$\sigma^{+/-}/\delta^{+/-}$ × RPTP$^{-}\sigma^{+/-}/\delta^{+/-}$). Pups were genotyped using PCR with gene-specific primers (Fig. 1*A*). Although each of the single knock-outs is viable at birth, live RPTP-σ/δ double mutants were not found in litters of newborn pups at